2022

Three-Dimensional Staging Series of Anolis Sagrei

Lilian Epperlein

LOYOLA UNIVERSITY CHICAGO

THREE-DIMENSIONAL STAGING SERIES OF *ANOLIS SAGREI*

A THESIS SUBMITTED TO

THE FACULTY OF THE GRADUATE SCHOOL

IN CANDIDACY FOR THE DEGREE OF

MASTER OF SCIENCE

PROGRAM IN BIOLOGY

BY

LILIAN EPPERLEIN

CHICAGO, IL

MAY 2022

ACKNOWLEDGMENTS

I would like to thank all the people who made this dissertation possible, starting with my amazing advisor Dr. Thomas Sanger, for his support, insight, advice, and mentoring throughout the development and completion of my research project. He was the invisible hand that nudged me on the right path, particularly when it came to the direction of this project and the voice of reason that got me out of many moments of impostor syndrome and self-doubt. I thank the members of my thesis committee, Dr. Martin Berg and Dr. Joseph Milanovich, for their advice and guidance. Your encouraging words and thoughtful feedback have been very important to me. I would also like to thank the graduate program director Dr. Terry Grande for always looking out for me and the other biology graduate students and always having our best interests in mind. I want to thank Joseph Schluep, for regularly providing μCT scanning assistance and for fixing the μCT scanner bed for me during a time when a replacement would've taken weeks to ship in.

Special thanks goes to all the Sanger lab people who aided in collections and processing. Hannah Maher, Jillian Schuberth, Alexandrea Turnquist, Gannon Cottone, Arlisse Lim, and Michelle Hajduk for egg collection. Alexandrea Turnquist helped with segmentation and three-dimensional model preparation. Go Team AnolisEvoDevo.

Many people have contributed to my wonderful experience at Loyola, including the Biology Department Faculty, the General Biology teaching faculty, and the departmental graduate students. I would like to thank the Department of Biology staff, especially Audrey

Berry and Virginia Lorenzo, for making the paperwork more bearable. Thanks to Dr. Megan Helfgott and Dr. Lisa Godsel for giving me the opportunity to teach general biology lab and mentoring me through the process. Biology graduate students, especially Erica Becker, Katherine Starr, Mike Vosburgh, and Manny Widuch, thanks for supporting me through these past few years, even if you didn't quite get my project. The comradery and group support pulled me through tough times.

To my friends and family that provided me with the motivation, encouragement and distractions required for completing this thesis project, I thank you. Finally, I want to thank my mother, Angelika Epperlein, for listening to me constantly rant and talk things out, for reminding me of my goals, and for the sacrifices you've had to make for me to pursue a master's degree.

TABLE OF CONTENTS

LIST OF FIGURES

ABSTRACT

With the rapid rise of Evo-devo and the concurrent development of new imaging techniques, comparative studies of development have accelerated over the last decade. Squamates, lizards and snakes, lack a traditional experimental model species for developmental investigations, yet are important for understanding fundamental evolutionary questions because of their remarkable diversity. However, several squamate species have growing communities of biologists building new resources for comparative and experimental studies of lizard development. Creation of detailed embryological atlases for these species will help promote their advancement. In the past, scientists have had to rely on destructive methods to take apart biological samples which allows them to visualize the three-dimensional (3D) anatomy.

However, X-ray computed tomography, CT scanning, allows for sub-10 micron, non-destructive imaging of vertebrate embryos. This technique allows not only the ability to analyze the hard tissues, but also, with the help of chemical counterstains, the ability to differentiate among soft tissues. I created a detailed, 3D embryological atlas of the model lizard species, *Anolis sagrei*, using micro-CT scanning. For a subset of stages I reconstructed the development of both hard and soft tissues, such as bone, muscle, and neural tissues. All reconstructions were performed in the free software package 3D Slicer. This anatomical atlas will be essential for future research on *Anolis* development, will build a comprehensive understanding of the embryonic development of anoles, and may provide a reference for people investigating the development of other lizards.

CHAPTER 1

INTRODUCTION

Over the past several decades Evolutionary Developmental Biology (Evo-devo) has impacted numerous and disparate biological fields including ecology, molecular biology, paleontology, and medicine (Bowler, 1996; Hall, 1992, 1999, 2002, 2003; Moczek et al., 2015). Evo-devo grew and matured by investigating the mechanisms that link genes to their structures (genotypes to phenotypes). This relationship is important because there is no one-to-one correspondence between gene and phenotype. Genes provide the road map, but they do not drive the embryo to its final destination. Hierarchical developmental processes unfold within the context of the environment to make structures with characteristics of size, shape, and color. Outside forces such as mechanical stimulus, environmental temperature and water, and interactions with chemical products will affect the genotype to phenotype transition (Hall, 2012).

Evo-devo allowed biologists to understand how the internal processes of development and natural selection combine to create morphological diversity (Wagner et al., 2000), whether that transformation is a minor modification in the shape of a bone or the origin of novel features such as the turtle shell (Burke, 1989, 1991; Gilbert et al., 2001), feathers (Prum & Brush, 2002), insect wings (Carroll et al., 1995; Weatherbee et al., 1999) or flowers with their striking color and shape (Hall, 2003; Simpson & Niklas, 1997). Model systems such as the fruit fly, mouse, zebrafish, and chicken are the most oft-used species in

Developmental Biology and formed the foundation of Evo-devo. Evo-devo grew out of the technical and cultural traditions established by developmental biology (Raff, 1996; Hall, 1999).

A major justification for the use of model species is that the biological phenomena that have been and are being uncovered can readily be extrapolated to other species, including humans (Jenner & Wills, 2007). Based on this, model systems, even those distantly related to humans (e.g., yeast, *C. elegans*, and Drosophila), have been prioritized by researchers and funding agencies (Hunter, 2008; Milinkovitch & Tzika, 2007). These traditional model systems have provided important and fundamental information on patterns and mechanisms of developmental change across the metazoan phylogeny. Yet ironically, one of Evo-devo's objectives is to understand the developmental and molecular bases of morphological diversity. This means that we must progress from the comfort of well-known model systems and venture towards non-traditional species to address diverse and distinct questions about their biological attributes (Sanger, 2012).

Thanks to the expansion of modern research tools such as the genome, transcriptome sequencing, and imaging, the use of non-model organisms used in developmental studies has greatly expanded. Non-model species used in developmental biology have played an important role expanding the field beyond the themes that catalyzed the field including: the effects of environmental neurotoxicants on fish development (Garcia et al., 2016; Siefferman & Hill, 2005; Ranasinghe et al., 2020); studying defects in the morphogenetic mechanisms involved in development of limbs responsible for the cessation of growth of limb buds in certain reptiles (Leal & Cohn, 2016; Raynaud, 1990); how inducing thermal stress affects rate of

developmental malformations in vertebrates (Chen et al., 2010; Piestun et al., 2009; Sanger et al., 2018, 2021) and the evolution of rapidly evolving sexual features (Hatlauf et al., 2021; Kaliontzopoulou et al., 2007; Murta-Fonseca et al., 2019; Oliveira et al., 2005; Sanger et al., 2013a). These discoveries, and others, offer a casual explanation for unique trends in morphological diversification, changes and perturbations in development associated with the environment, and the evolutionary form (Carroll, 2008; Carroll et al., 2005). One of the fundamental tools of developmental biology is a description of the normal stages that define standard divisions of embryogenesis and morphogenesis. These staging series include pictures and descriptions that define the standard divisions of development that are used by the community of biologists studying that organism (Hopwood, 2007). They can also be used as reference for investigators studying closely related species (e.g., Sanger et al. 2008, Griffing et al. 2019). Staging series have played an important role as the standard for comparing both experimentally perturbed embryos to the reference and as a standard for comparisons among even distantly related species. For example, in a recent study of embryonic thermal stress affects the *A. sagrei* staging series (Sanger et al. 2008) was used to identify changes in the rate of development and origin of craniofacial malformations in embryos (Sanger et al., 2018, 2021). Staging tables also provide a valuable reference that allows an investigator to know what stages are forming at what times during development, an especially valuable resource for embryos that cannot be readily observed (e.g., oviparous species). Embryological tables have been created for all of the commonly used vertebrate species in Developmental Biology, such as the mouse *Mus musculus* (Downs & Davies, 1993; Theiler, 1972; Wong et al., 2012), chicken, *Gallus domesticus* (Arnaout et al., 2021; Hamburger & Hamilton, 1951; Stern, 2018), zebrafish,

Danio rerio (Kimmel et al., 1995; Parichy et al., 2009), and frog *Xenopus* (Phipps et al., 2020). They are also commonly used for a large number of less well-known developmental models such as Savigny's treefrog *Hyla savgnyi,* ornate narrow-mouthed frog *Microhyla arnata,* grey balloon frog *Uperodon glublosus,* ornate pigmy frog *Microhyla fissipes* (Degani, 2015; Narzary & Bordoloi, 2013; Wang et al., 2017), Axolotl *Ambystoma mexicanum* (McCusker & Gardiner, 2011; Roy & Gatien, 2008), and African house snake, *Boaedon fuliginosis* (Boback et al., 2012) as partial or complete tables.

Embryonic development is a continuous process where the embryo undergoes a consecutive series of tissue-specific cell differentiation, morphogenesis, and growth until the organism reaches maturity. This continuous change can be analyzed by treating it as a series of developmental events, or developmental stages if you will. The order at which morphological stages take place is known as a developmental sequence and are of interest because they define the ontogeny of the individual (Gould, 1982; Gould, 1977; McKinney, 1991; Smith, 2001). Changes in developmental stages, therefore, reflect evolutionary changes in development and likely give a strong indication about the origins of morphological diversity. Constructed tables also aid in establishing patterns of relationship amongst species by identifying homologous structures and helping investigators establish when and where in development changes arise. Classification of development into distinct, definable stages allows embryos to be compared more easily to the reference, especially in the case where embryos are experimentally treated. Also, developmental events are inter-dependent so that the competence of a tissue to respond to a specific signal could be dependent on the stage of development, and can change dramatically within a very short

time (Dias & Schoenwolf, 1990; Stern, 2018; Storey et al., 1992; Streit et al., 1997).

Effective methods of visualizing embryonic phenotypes have become crucial to the expanded utility of new and emerging model systems. Historically, phenotyping of embryonic morphology includes visualization techniques such as serial histological sectioning and light microscopy, which are both time consuming, may destroy the embryonic sample, and cannot visualize the inner tissue architecture of the embryo. For example, histology uses thin slices of embedded embryological material, which then needs to be manually sectioned. Because of this, these histological approaches can also introduce distortions on the final three-dimensional image (3D) due to the sectioning process (Cleary et al., 2011). Recently, nondestructive techniques, such as X-ray computed tomography (CT), have come to the forefront have further enhanced the analysis of embryological phenotypes (Ding et al., 2019; Wong et al., 2012).

X Ray Computed Tomography

Recently, non-destructive visualization techniques have come to the forefront for whole- volume imaging of animal tissues. One such technique, X-ray computed tomography (CT), has become an attractive option for analyzing morphological phenotypes because it allows for 3D visualization of biological structures which examine tissue anatomy of living, preserved, and fossil species. Morphological studies harnessing X-ray imaging techniques, including standard CT (greater than 100µm resolution), micro-CT (5-100µm resolution), and nano-CT (150nm and 50µm) provide volumetric models for mineralized hard and soft-tissue anatomy which have far surpassed those of other non-destructive visualization methods (Gignac et al., 2016; Metscher, 2009a, 2009b; Neu & Genin, 2014).

Figure 1. Diversity of species' skeletons illustrating the utility of CT scanning. Phylogenetically and morphologically diverse examples of CT imaged organisms that display hard tissue, such as bone or exoskeleton, as 3D volumes. Specimens are leopard seal *Hydrurga leptonyx* (USNM 270326), spotted hyena *Crocuta crocuta* (USNM 181527), American alligator *Alligator missipiensis* (OUVC 11415), northern snapping turtle *Elseya dentata* (TMM:M 9315), large seed harvesting ant *Pogonomyrmex desertorum* (UTEP:ENTO 4702), no common name *Eupolybothrus liburnicus* (CBSS:CHP 538), lined seahorse *Hippocampus erectus* (TCWC:ICHTHYOLOGY 13069.01), no common name *Mabea speciosa* (USNM 000368389), and Texas horned lizard *Phrynosoma cornutum*. Data was publicly available through Morphosource or collected at LUC.

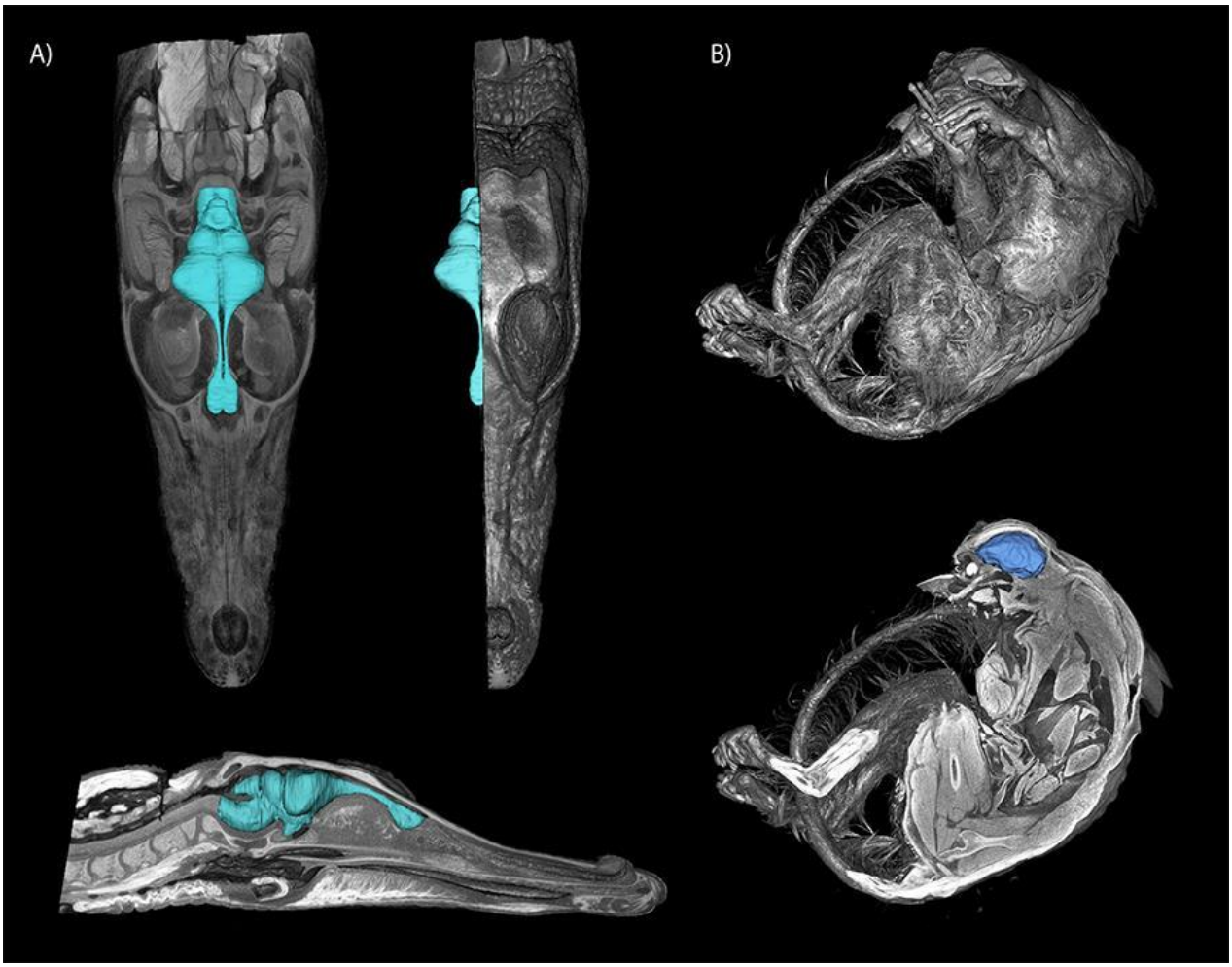

Figure 2. Diversity of species' skeletons illustrating the utility of soft-tissue CT scanning. Vertebrates imaged using iodine-based contrast enhanced computed tomography (DiceCT), demonstrating the diversity of soft tissue anatomy, such as the brain and muscle, that can be visualized using CT scanning. Brains of both vertebrates were segmented, and 3D rendered at LUC. Specimens are (a) saltwater crocodile *Crocodylus porosus* (OUVC 10899) (b) thick-tailed galago *Otolemur crassicaudatus* (DLC 1715f). Specimen scans were accessed using publicly available data from Morphosource.

CT imaging was initially developed to visualize hard tissue, such as bone. Non-mineralized soft tissue structures cannot be readily visualized using conventional x-ray imaging techniques. However, the increasing availability of CT resources have led researchers and medical professionals to advance innovative means to overcome this challenge. Simple staining methods that allow for high contrast imaging by increasing the radio densities of soft tissue so that their visualization in CT is comparable to or better than that of naturally mineralized tissues (Gignac et al., 2016; Harris et al., 1979; Metscher, 2009a, 2009b; Wallingford, 1953). Currently, several contrast-enhancing staining agents are used for soft-tissue specificity and radiopacity, such as: iodine (I_2KI or Lugol's solution); (Degenhardt, et. al. 2010; Gignac et al., 2016; Metscher, 2009a, 2009b), phosphotungstic acid (PTA) (Metscher, 2009a, 2009b; Pauwels et al., 2013), Osmium tetroxide (OsO_4) (McDowell & Trump, 1976; Metscher, 2009a, 2009b; Mizutani & Suzuki, 2012; Pauwels et al., 2013) and phosphomolybdic acid (PMA) (Pauwels et al., 2013). The utility of each stain depends on the size of the specimen and composition of tissue being imaged.

Among these effective contrast agents, Lugol's iodine, also known as strong solution of iodine-potassium iodide (I_2KI), has become the popular choice amongst anatomists and morphologists due to its simple protocol, cost effectiveness and differential affinities for different types of soft tissues. Lugol's iodine can be used to visualize soft tissue anatomy in invertebrates, vertebrates, and their embryos (Metscher, 2009b, 2009a). Phosphotungstic acid (PTA) staining is as robust as Lugol's and produces excellent contrast among tissues but cannot penetrate into deep tissues more than a few millimeters in size.

This makes PTA ideal for staining smaller tissues, but not for large, or adult specimens (Dunmore-Buyze et al., 2014; Lesciotto et al., 2020; Metscher, 2009b, 2009a). Large-scale, publicly funded, digitization projects such as #ScanallFish and oVert (Open Exploration of Vertebrate Diversity in 3D), are generating high-resolution micro and nanoCT scans of thousands of vertebrates. Data from these projects are shared with the community using 3D specimen repositories such as Morphosource, through various open, creative common licenses (Degenhardt et. al. 2010; Gignac et al., 2016; Gignac & Kley, 2014; Holliday et al., 2013; Lautenschlager et al., 2014; Metscher & Müller, 2011; Schwarz et al., 2016).

Researchers from many biological disciplines now use high-resolution, three-dimensional models demonstrating a wide range of taxonomic and anatomical detail. Such data, where 3D digital renderings of objects such as bones have rapidly advanced, can now be produced less expensively and more quickly than ever before. While software for processing CT data was once cost prohibitive, newer open-source software allows for more people the ability to analyze three- dimensional data. Quickly generated high-quality raw data on morphology now presents new opportunities where researchers can improve their proficiency in studying a specimen using 3D virtual ‘specimen data’ (Giribet, 2010; J. J. Shi et al., 2018; Ziegler et al., 2010). Morphosource (Boyer et al., 2016; Boyer et al., 2014), Morphobank (O’Leary & Kaufman, 2011), and Digitalfishlibrary (Berquist et al., 2012; Eichberger et al., 2006) have made 3D versions of specimens increasingly available. Researchers who lack physical access to a particular specimen can utilize 3D digital versions of the specimen without ever seeing the specimen first-hand. Furthermore, web-accessible digital libraries for rendered three-dimensional models have been developed.

Sketchfab, one such volume viewer, allows authors to intuitively upload models, define rendering options (lighting, material properties, etc.), provide supplementary annotations, and share models with research collaborators and educational classrooms (Hagmann, 2018; Nesbit et al., 2020; Tiznado-Matzner et al., 2019).

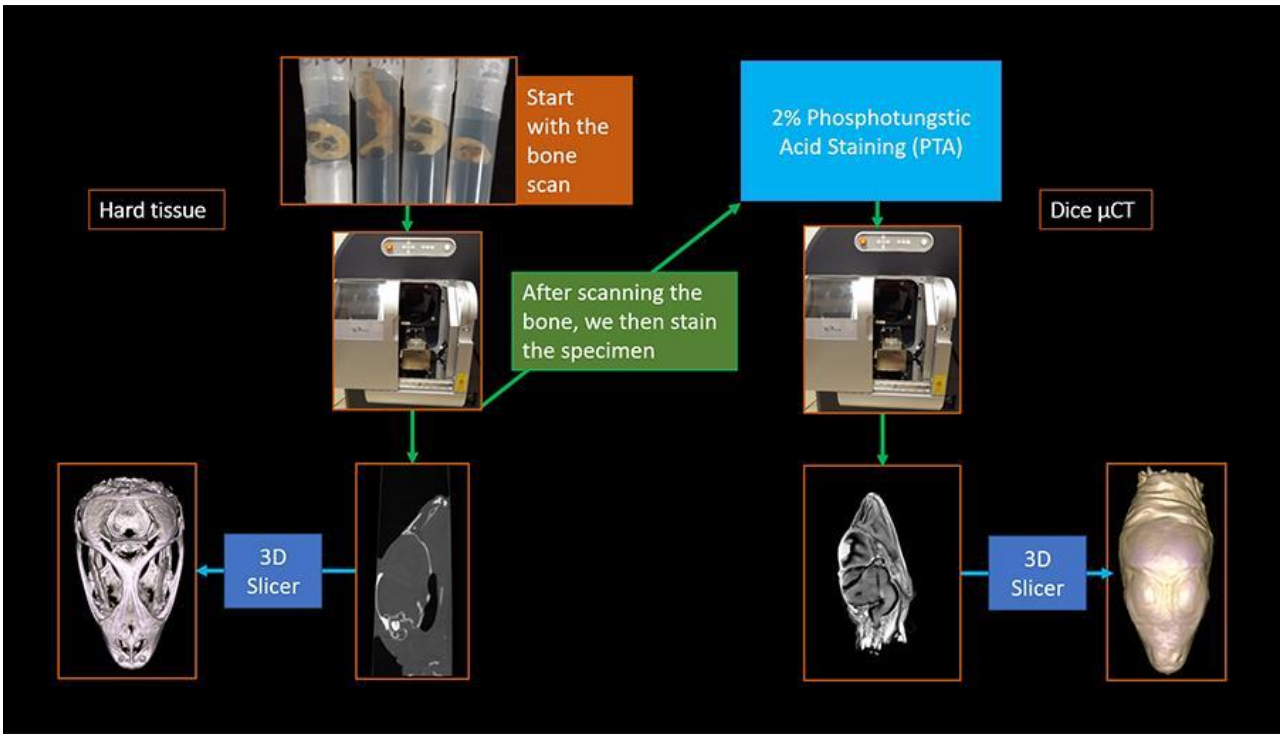

Figure 3. Workflow chart demonstrating the process of µCT scanning hard tissue and DiceCT scanning.

Software

CT scanning generates hundreds to thousands of cross-sectional views (i.e., projections) of the specimen. These projections can then be viewed as individual TIFF or DICOM images or turned into three-dimensional image reconstructions (Pointer, 2008; Shi et al., 2020). DICOM files contain a header file that includes details about the scan but are not a functionally different form of data than TIF images. Many CT reconstruction packages are on the market, however these programs often have a non-intuitive user interface for most biologists or are too expensive for many labs to purchase (often over $10,000; Shi et al., 2020). However, research teams have developed freely available, open-source image reconstruction applications, such as 3D Slicer, Dragonfly, and ImageJ. These toolkits are free and not tied to a specific hardware.

Squamates: Emerging Models for Developmental Biology

Amniota is an evolutionary clade of vertebrates that includes all living reptiles, mammals, birds and their extinct relatives and ancestors. This lineage is characterized by the presence of amniotic egg, which have membranes that protect the embryo from desiccation, acting as a cushion to protect the embryo, promote gas transfer, and store waste materials (Benton et al., 2015; Laurin & Reisz, 1995). Our current understanding of amniote embryogenesis primarily derives from studies in mice and chick model systems, only two representatives of the approximately 25,000 species of amniote (Diaz et al., 2017; Hedges, 2012). This exclusive focus on embryos from model organisms has led to low coverage of biodiversity, making it difficult to test hypotheses about anatomical diversification and developmental evolution (Sanger & Rajakumar, 2019).

Squamates, lizards and snakes, are particularly important for understanding the mechanisms of anatomical diversification in vertebrates because of their high diversity and unique suite of evolutionary adaptations (e.g., snake fangs, adhesive toe pads, and limb lessness; Gray et al., 2019; Jensen et al., 2013; Losos, 1990a, 2009; Sanger, 2012; Sanger & Kircher, 2017; Yaryhin et al., 2021). They constitute a major vertebrate radiation, representing almost a third of all known amniotes by more than 10,000 species (Uetz & Stylianou, 2018). And although specious, they remain an underrepresented group in developmental studies. This brings with it problems for questions looking into evolution of digit and limb loss, developmental transitions of the head, gene ontology or understanding gene regulation and expression patterns in reptiles among others (Bininda-Emonds et al., 2007; Chang et al., 2009; Rasys et al., 2019, Sanger et al., 2018).

There has not been a single taxon of lizard that has been adopted among reptilian based laboratories as the developmental model to study. This likely reflects the interest of this community in understanding squamate diversity rather than probing deep into the depths of cellular and molecular biology of reptiles. Over the past two decades, there have been a handful of lizard taxa that have been documented and proposed as useful developmental models. First, Sanger et al. (2008) proposed *Anolis sagrei* as a developmental model for squamates (Sanger et al., 2008). Serving as more than a single developmental model, *A. sagrei* could provide an experimental anchor for *Anolis* to serve as a model clade, investigating the subtle ecomorphological differentiations within the adaptive radiation (Sanger et al., 2008; Sanger & Rajakumar, 2019). Wise et al. (2009) described the embryogenesis in the *Eublepharis macularius*, the leopard gecko, a well-known reptile

amongst herpetoculturalists and has been used in a wide range of studies including tissue grafts and tail regeneration. Ollonen et al. (2018) describing the complete post-oviposition embryonic development for *Pogona vitticepts,* the bearded dragon, which, have experienced independent radiations and are part of a diverse lizard group, the Australian agamids. Finally, Griffing et al. (2019) described the development of the mourning gecko, *Lepidodactylus lugubris*, a parthenogenetic species, composed entirely of females and reproduce without male gametes. This species will serve as model for comparative studies of sexual evolution among geckos and their unique patterns of morphological and sexual evolution. These studies have demonstrated the immense utility of squamates as models for development.

Anolis

Anolis lizards, or anoles, are one of the largest vertebrate genera, containing nearly 420 species (Losos, 2009). Native throughout the northern half of South America, the Caribbean, and Central American, anoles have been introduced on Pacific islands including the Bermudas, Hawaiian Island, Taiwan, and the Bonin Islands. Anoles are relatively small, often arboreal insectivores, but interspecies variation exists in size, habitat and diet (Losos, 2009). As a textbook example of adaptive radiation, anoles are known for occupying different ecological niches, resulting in replicated patterns of morphological evolution on different islands of the Greater Antilles (Losos, 1994; Poe & Anderson, 2019; Sanger & Kircher, 2017). The repeated evolution of anoles offers the opportunity to test many generalizations about evolutionary processes. Over the past 50 years, anoles have become one of the most widely-studied model systems for studies of reptile evolution, ecology,

behavior, physiology, genomics, and development (Rasys et al., 2019; Sanger et al., 2008; Sanger & Kircher, 2017). A Google Scholar search for *Anolis* recovers over 27,000 articles that have been published since 1980 and over 16,000 since 2010.

Anolis species inhabiting the Greater Antilles islands are a classic example of convergent evolution (Langerhans et al., 2006); termed ecomorphs – species that are not close phylogenetically are similar in morphology, ecology, and behavior (Williams, 1972, 1983; Losos, 1994; Losos & Schneider, 2009). Anole faunas have been noted for their abundance and diversity and the corresponding diversity of the microhabitats in which they occur but also by the conspicuous presence of highly similar species from one island to another (Williams, 1983). The similarity among species within each ecomorph category is striking, converging on color, size, body proportions, perch and foraging and escape behavior and that these are ecological analogues. As such, the radiations have produced essentially the same set of ecological types of ecomorphs on each island (Losos, 1994; Rand, 1969; Schoener, 1988; Williams, 1972, 1983). Six *Anolis* ecomorphs have been defined based on morphology and habitat: limb length, dimensions of adhesive toe pads, tail length and the dimensions of the skull (Beuttell & Losos, 1999; Glossip & Losos, 1997; Irschick & Losos, 1998, 1999; Losos, 1990, 1990b, 2009; Losos & Sinervo, 1989; Williams, 1972). Because of this multidimensional convergence, each of these traits is thought to be adaptive according in their respective microhabitats which range from grasses, open ground, and different parts of trees of respective anoles. This unique assortment of environmental pressures within each microhabitat are proposed to drive adaptation within each microhabitat and thus the emergence of convergent species assemblages (Losos et, al.,

1992, 2009; Losos & Ricklefs, 2009).

Given the extensive ecological and evolutionary understanding of anole radiations, anoles have become an excellent model clade to study the development of both ecological and evolutionary relevant morphological changes (Campbell-Staton et al., 2017; Gorman & Hillman, 1977; Gunderson & Leal, 2012; Hertz et al., 1979; Huey & Bennett, 1987; Huey et al., 2009; Muñoz et al., 2014; Sanger et al., 2018). The genome sequencing of *Anolis carolinensis*, the green anole, allowed for a deeper understanding of amniote evolution, opening the doors to experimental embryology and functional genomics (i.e., knock-down or overexpression studies), and brought new attention to this genus by those traditionally trained in Developmental Biology (Alföldi et al., 2011; Geneva et al., 2021; Sanger & Kircher, 2017). Research of anole development has expanded greatly beyond the traditional evolutionary utility of the genus including studies of heart development (Jensen et al., 2013; Koshiba- Takeuchi et al., 2009), tail regeneration (Hutchins et al., 2014, 2016; Ritzman et al., 2012), longitudinal body axis formation (Eckalbar et al., 2012; Kusumi et al., 2013), external genital (i.e., phallus) development (Gredler et al., 2014, 2015; Infante et al., 2015; Tschopp et al., 2014) and new tissue and ex-ovo embryo culturing techniques (Diaz & Trainor, 2015; Park et al., 2014; Sanger & Kircher, 2017; Tschopp et al., 2014). More recently, advances in CRISPR-Cas9 genome-editing technology in both model and non-model species (Bassett et al., 2013; Gilles & Averof, 2014) demonstrate that the microinjection of CRISPR-Cas9 into unfertilized oocytes is an effective method to produce targeted mutations in *A. sagrei* (Rasys et al., 2019). Whether those studies are within species, among closely related anole species, or as a representative squamate for

comparisons among distantly related amniotes, anoles are providing a framework for testing evolutionary, developmental, and genomic hypotheses at different phylogenetic scales (Sanger & Rajakumar, 2019).

Following from years of concentrated study on *Anolis* lizards by the Sanger Lab and others, within this thesis I will describe a detailed post-oviposition, three-dimensional staging atlas for the body and head of *A. sagrei* based on external morphological characters previously defined by Sanger et al. (2008). Using non-destructive μCT techniques for embryological characterization, I track limb, craniofacial, and neural development. I also describe the cranial ossification sequence, since an easily available, complete morphological description of the embryonic skull is still lacking for most lizard families, including anoles. The data generated, such as images and 3D mesh files, will be globally open for exploration, download, and 3D printing on anolisevodevo, Morphosource, and Sketchfab. Additionally, the data generated will be a great resource for future evolutionary and developmental investigations in squamates and the continued study of *A. sagrei* as a model for evo-devo.

CHAPTER 2

METHODS/MATERIALS

Here I describe protocols for the construction of a novel 3D embryonic staging table for the head and body of *A. sagrei* based on µCT imaging. I collected multiple embryos of each developmental stage (Sanger et al. 2008) and nondestructively tracked the limb, craniofacial, and neural development along with the sequence of craniofacial ossification. This was possible by employing µCT imaging for hard tissue and contrast-enhanced dice µCT imaging using contrast staining agents. I rendered these scanned embryos and tissues of interest in order to create interactive 3D models that can be used in both research and education.

Husbandry

I followed the protocols for husbandry and embryo collection of A*nolis* lizards that are described in detail in Sanger et. al. (2008). Approximately 200 gravid *A. sagrei* females were transported from Miami, FL to Loyola University Chicago, IL in May 2019 and again in 2020. I housed four to six gravid females per cage. Over the summer months, I checked the cages daily for eggs, ranging from 2-36 eggs per day. In short, cages were maintained in climate controlled walk-in chambers kept at 28.5°C with misting regularly occurring every two hours to maintain humidity and provide drinking water for the lizards. A small pot was stationed in every cage which was filled with moist soil for females to lay their eggs. I

checked these pots between the hours of 8:00 am – 10:00 am daily for egg collections, as well as the surrounding areas around the pot. The collected eggs were incubated with moist vermiculites, and placed in sealed petri dishes which were kept in a humidified incubator at 27°C.

Specimen Collection

There are a total of nineteen described stages for *A. sagrei* (Sanger et al., 2008). Early cleavage or gastrulation stage embryos were not described in Sanger et. al. (2008) because these stages occur within the oviduct of the gravid female. Therefore, the earliest stage that I collected were, Sanger Stage 4, the time of oviposition. Stage 4 corresponds to the stage at the “early limb- bud" stage of development and Stage 19 corresponds to the stage that precedes hatching from the egg.

I acquired multiple embryos at different developmental stages, ranging from stages 5 to 19. I then dissected the eggs using #5 watchmaker’s forceps and 3mm iris scissors under a dissection microscope. During the dissection process I immersed the eggs in cell-neutral 1% phosphate buffered saline solution to keep the embryos from becoming deformed. I identified the developmental stages of *A. sagrei* using the developmental staging series for the lizard genus *Anolis* as a guide (Sanger et al., 2008). Key morphological characteristics such as limb morphology and growth, scale development, facial prominence and development, and body pigmentation were used to identify the various stages.

I fixed embryos in 4% phosphate-buffered paraformaldehyde, dehydrated in graded methanol, and stored in a 4^{o}C freezer until future use. Embryos stored in methanol underwent a rehydration phase to PBS. Following rehydration, I post-fixed samples in 1%

glutaraldehyde at 4°C for 24 hours. Following fixation, I then washed the samples with PBS and dehydrate them to 70% ethanol. Some embryos were immediately prepared for scanning and were fixed directly in 1% glutaraldehyde at 4°C following dissection. Samples would then follow the same dehydration steps as mentioned above.

CT Scanning: **Hard Tissue Preparation Protocols**

I acquired high-resolution µCT scans of embryonic skull bone development at Loyola University Chicago in the Department of Biology imagining facility using the Perkin Elmer Quantum GX2 µCT scanner. To visualize skull bone development, I first scanned unstained specimens. Because I did not yet know when the first skeletal elements form, I began with embryos at Stage 9. Any movement during scanning, including shrinkage associated with desiccation, would create blurring and a misalignment of the center of rotation, which would result in poor or unusable data (e.g. blurry edges, or cut out limbs within two-dimensional (2D) tomography slices). Therefore, after dehydration (above) I embedded all specimens in 0.5% low gelling temperature agarose for scanning within a 1ml pipette tip with its tip flame sealed. Embedding in agarose, allowed me to suspend the embryo and prevent embryo deformation (Metscher, 2009b). Specimen were left for a minimum of 57 minutes for both hard and soft tissue CT scans.

I performed full body and head scans separately where I would melt and resubmerge specimens in agarose over the course of scans. To remove the specimen from agarose, I suspended the agarose filled micropipette in the holes of a heating block that was filled with water till the agarose returned to a liquid state. Once the agarose was melted, I cut the tip of the micropipette and poured the embryo and the liquid agarose into a beaker filled with PBS. I then washed the embryo of any remaining agarose and dehydrated from 50% to 70% ethanol for future use. I did not embed late embryos (i.e., after scale formation) in agarose because they were too big to fit in the micropipette and at those stages scale formation has begun which allows them to be scanned before drying out or desiccation can occur. Due to that, late-stage embryos were placed in in small zip lock bags for scanning.

CT Scanning: **Staining Protocols**

After skeletal scans were completed, I prepared the same specimens for contrast-enhanced scanning. To prepare anole embryos for contrast scans I first fixed and dehydrated them to 70% ethanol. I found that certain staining protocols were more favorable based on size and age of specimen and density of tissue. I stained embryos at different concentrations of iodine and PTA to properly identify the best contrast-enhanced data, stain durations. All staining lasted 24 hours. I discovered that using Lugol's iodine as a contrast agent for early-stage specimens (5-14) embryos did not provide adequate staining (including higher concentrations of iodine). Instead, I used phosphotungstic acid (PTA; Metscher, 2009b, 2009a) to stain early-stage specimens overnight in 2% PTA in 70% ethanol. Conversely, I stained late-stage embryos (15-19) with Lugol's iodine (I_2KI) overnight using 3.75% Lugol's iodine in 70% ethanol for 24-48 hours, till the skin of adequately stained specimens was a dark amber color.

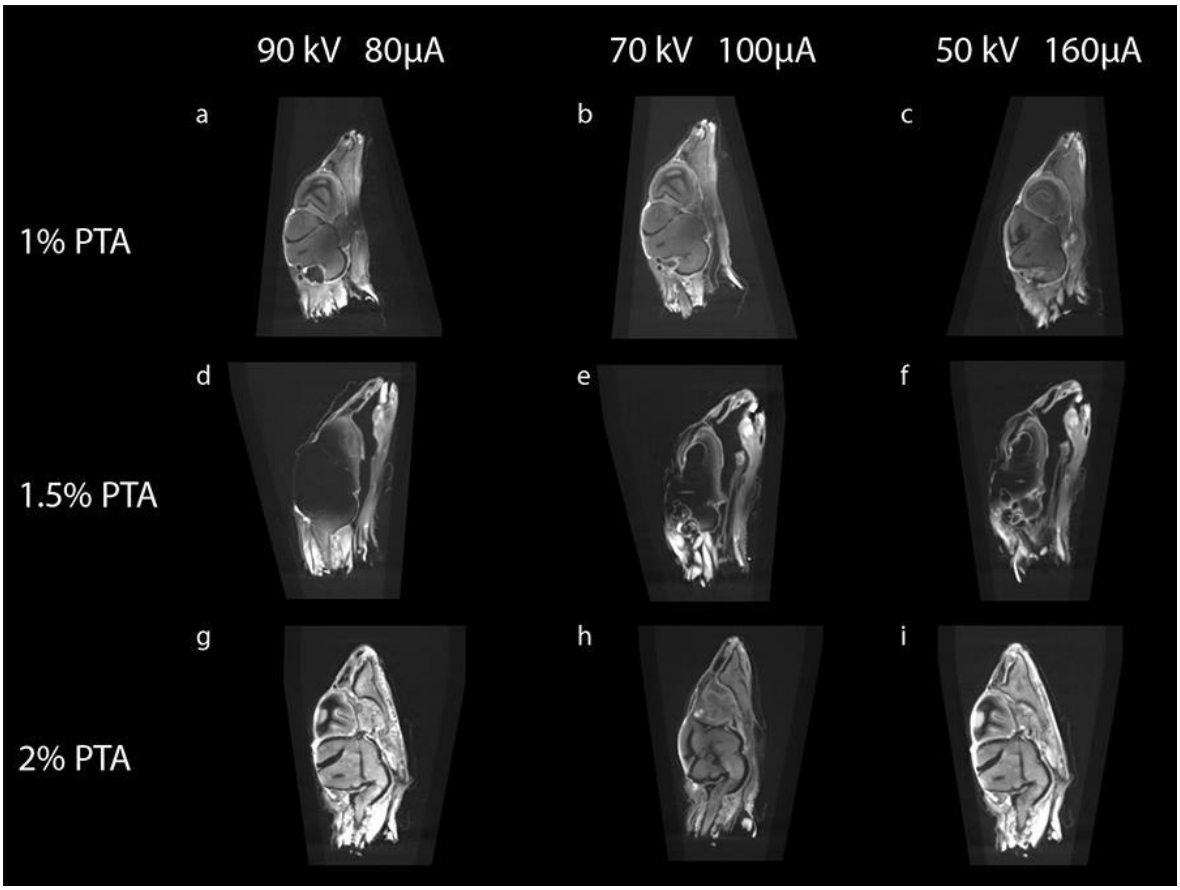

Figure 4. Effects of PTA stain concentration on specimens. Course of the concentration of PTA staining solution and kilovolt/microamp CT scanning intensity varies with the degree of image quality. Three hatchling stage anoles were stained with varying PTA concentrations and scanned by micro-CT with different scanning intensities. Representative sagittal MPR images from the three hatchlings are shown. (A-C) Saturated 1% PTA and (D-F) 1.5% PTA fails to penetrate specimens fully but does show progressive diffusion of PTA into the tissue. (G-I) 2% PTA solution shows good penetration and scanning intensity, especially for (I) and (G).

Scanning Parameters

I conducted hard and soft tissue scans at 50 kilovolts (kV), 160 microamperes (µA), 18 µm voxel size, with a 0.05 mm Aluminum (Al) filter. I reconstructed raw tomography projections using the Quantum GX2 µCT imaging system which generated approximately 500 cross-sectional images in digital imagining and communication in medicine file format (DICOM) per data set. For visualization of these data sets, I imported them into 3D Slicer version 4.11.0 (2019, 3D Slicer, Seattle, Washington State) where I compiled them into 3D renders for segmentation and anatomical analysis.

Data Processing

I processed segmentations in 3D Slicer (www.slicer.com), an open-source magnetic resonance imaging/computed tomography analysis program (Fedorov et al., 2012). I uploaded DICOM files into 3D Slicer as a volume, I then adjusted the range of the x-ray spectrum the files to capture the desired structures, used a combination of filters to obtain a smooth image that maintained anatomical detail. 3D Slicer has a variety of packages to conduct image segmentation (Fedorov et al., 2012). Once the file has been uploaded to 3D Slicer and adjusted the range of the x-ray spectrum to the desired anatomical structure voxel intensity, I used embedded filters of 3D Slicer to render volumes and visualize bone, reduce volume noise and static shown in the 3D renders, and to smooth out static on the surface mesh of scanned volumes. I applied different filters based on the type of scan data, skeletal or soft tissue μCT. The filters I applied to skeletal scans are shown in Figure 4: Medianimagefilter, used as a robust approach for noise reduction and then Absimagefilter to compute the absolute value of each pixel. Soft tissue μCT scans tended to have more noise and artifacts, which resulted in images shown above in Figure 6. By applying the Gaussian Blur Image filter, I was able to create models with smooth surfaces.

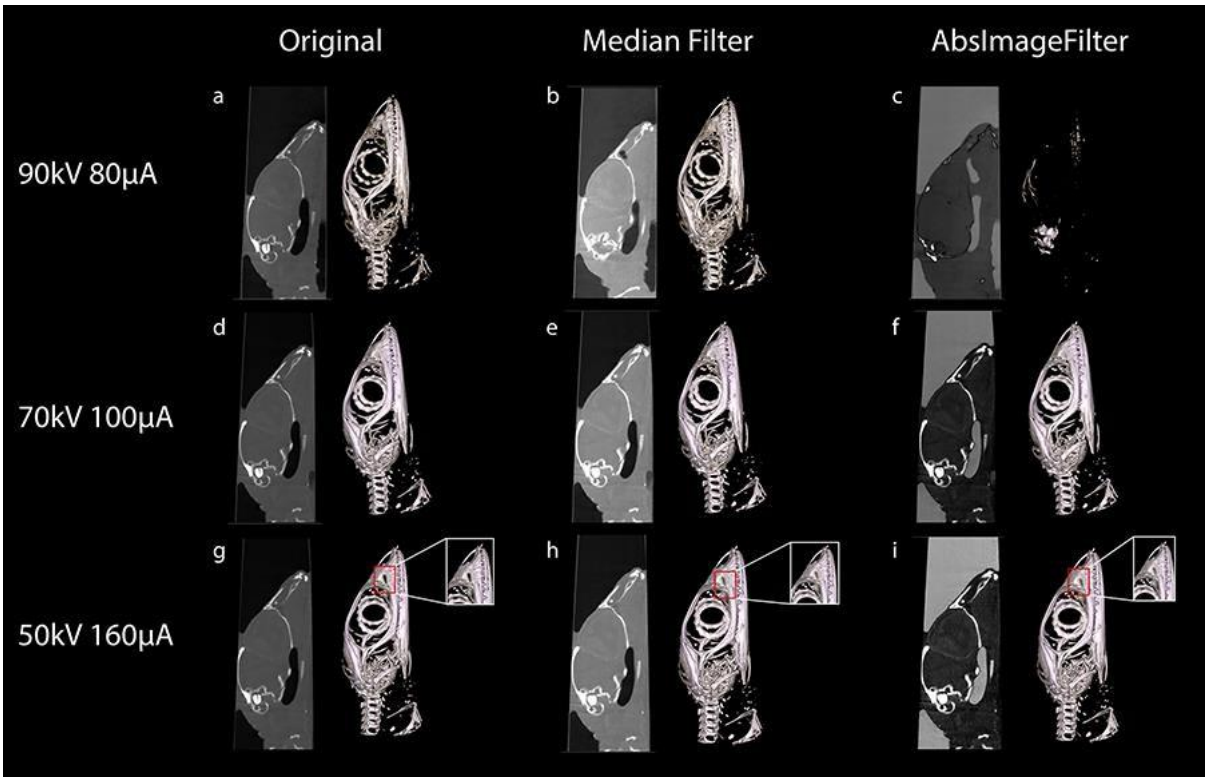

Figure 5. 3D Slicer filters applied to CT scanned samples. A course of filters applied to samples that were scanned at various kilovolt/microamp CT scanning intensity to study the degree of image quality. Three hatchling stage anoles were scanned by micro-CT with different scanning intensities. Representative sagittal MPR images and 3D renders from the three hatchlings are shown. (A-C) Scanned at 90kV and 80µA, and (D-F) 70kV and 100µA fail to capture bones fully from initial scans and even after filters were applied to the raw data, the bone fragments either disappear entirely or do not produce the same quality as the raw data produced from G-I. (G-I) 50kV and 160µA shows good penetration and scanning intensity; filter were applied: Medianimagefilter, used as a robust approach for noise reduction and Absimagefilter to compute the absolute value of each pixel. These filters further distinguish bones in the two-dimensional (2D) computed tomography images.

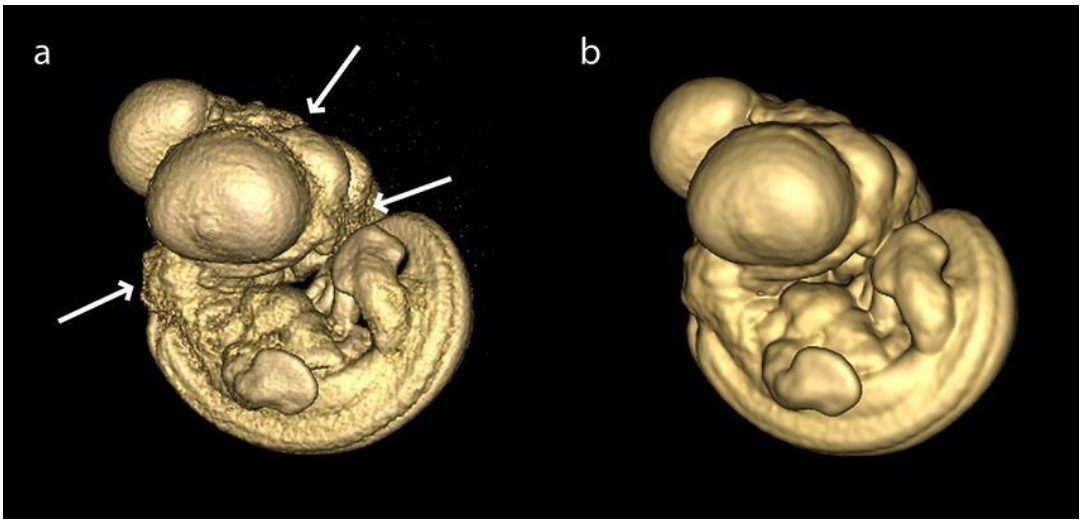

Figure 6. 3D render of scanned embryo before and after applied filters. A 3D volume render of a CT scanned embryo (Stage 7). (a) Original volume render using 3D Slicer and (b) after the Gaussian Blur Image Filter has been applied to the volume render.

3D Slicer possesses, Segment Editor, a module which offers a wide range of segmentation methods. Once the appropriate filters were applied, I used the Segmentation editor's mixture of tools: "threshold", "scissors", "eraser" and "paint" to make 3D arrays of voxels, for both segmenting out bones in skeletal scans and the soft tissue in μCT scans. This was done by applying a tight grayscale thresholding to all image slices around the desired structures and avoid capturing undesired structures. However, due to these structures having thin bone densities or dense tissue stains, the grayscale threshold would still register undesired structures or not capture desired structures completely, which made it necessary to also "paint" by hand through all the slices. A 3D model was then generated, which could be freely moved on the screen and viewed from all perspectives.

To create a virtual interactive 3D model that could easily be manipulated and shared, I exported an OBJ file from 3D Slicer. I then uploaded this model to the website Sketchfab (www.sketchfab.com) so that the 3D models created could be viewed and manipulated on the web.

CHAPTER 3

RESULTS

I described cranial and brain morphology of *A. sagrei* embryos from oviposition to hatching using microCT to produce 3D models. There are nineteen post-oviposition developmental stages described for *Anolis sagrei* (Sanger et al. 2008), for which I describe 18. Early development, including cleavage, gastrulation, and early organogenesis (including Sanger stages 1- 3), occur in the oviduct of the females and were not assessed in my study. Later stages are defined based on the progression of pigmentation and scale development. However, these structures could not be visualized in my CT data. Therefore, I staged these embryos under a light microscope before scanning. Herein, I describe the staging body, head, brain, and skull using μCT and staining with PTA (Figure 8-13).

Whole Embryo

Stage 5: Late Limb-Bud

Limbs: Both fore and hindlimbs are wider than they are long. The hindlimb buds are slightly larger than the forelimbs.

Upper Jaw: Fronto-nasal prominence (the area of where the face will form anterior to the telencephalon) is prominent. Maxillary processes are small not extending beyond the anterior eye.

Lower Jaw: Mandibular process extends rostrally.

Eye: Differentiation of Lens.

Stage 6: Paddle-shaped Bud

Limbs: Distal limbs are both paddle shaped.

Upper Jaw: Maxillary process extends rostrally, extending beneath the telencephalon. Fronto- nasal process is now present, appearing bifurcated into two large projections.

Lower Jaw: Mandibular processes roughly at level with center of eye.

Eye: Continued differentiation of lens. No eyelid visible.

Stage 7: Digital Plate

Limbs: Paddles are wider than in previous stage. Medial digits have begun to condense. This is most obvious on the hindlimb. There is now a notable 90-degree flexion at the elbow and knee. *Upper Jaw:* Maxillary processes nearly reach the underside of fronto-nasal process. The bifurcation of the fronto-nasal processes appears reduced.

Lower Jaw: Extension of mandibular process to anterior margin of eye.

Eye: Optic cup ovoid in shape.

Stage 8: Digital Condensations

Limbs: Condensation of digit cartilages are visible with slight thinning of internal webbing, but no regression. Proximal limb joints have become more distinct.

Upper Jaw: Maxillary process is in contact and may begin to fuse with fronto-nasal process.

Lower Jaw: Mandibular process extends rostrally to anterior edge of eye.

Eye: Optic cup still ovoid in shape. The earliest signs that the ectoderm is growing over the eye to become an eyelid is apparent.

Stage 9: Early Digital Web Reduction

Limbs: Reduction of interdigital webbing is beginning, freeing the digit tips. Fourth digit now noticeably longer than other digits.

Upper Jaw: Fronto-nasal process and maxillary processes now fused creating first evidence of a forward-facing snout anterior to eye.

Lower Jaw: Mandible still not level with the snout.

Eye: Upper and lower eyelids now distinct covering 10% of the eye.

Stage 10 Digital Webbing Partially Reduced

Limbs: Interdigital webbing has reduced by half its length on digits but remains clearly visible between the medial digits. Differential elongation of the medial digits continues.

Upper Jaw: Upper jaw is of equal length to lower jaw.

Lower Jaw: Lower jaw is of equal length to upper jaw.

Eye: Eyelids cover 25% of the eye.

Stage 11: Digital Webbing Completely Reduced

Limbs: Digital webbing has fully regressed. Pinching at distal tips provides first evidence of claw formation.

Eye: Eyelids cover 75% of the eye.

Stage 12: Digital Pads

Limbs: Further pinching at distal tips.

Eye: Half of eye covered by eyelids.

Stage 13-19:

These stages are defined based on characteristics of scale and pigmentation development, which are not visible in the CT scans. I have included the body and head images in Figure 7 as reference for later descriptions of brain and skull development.

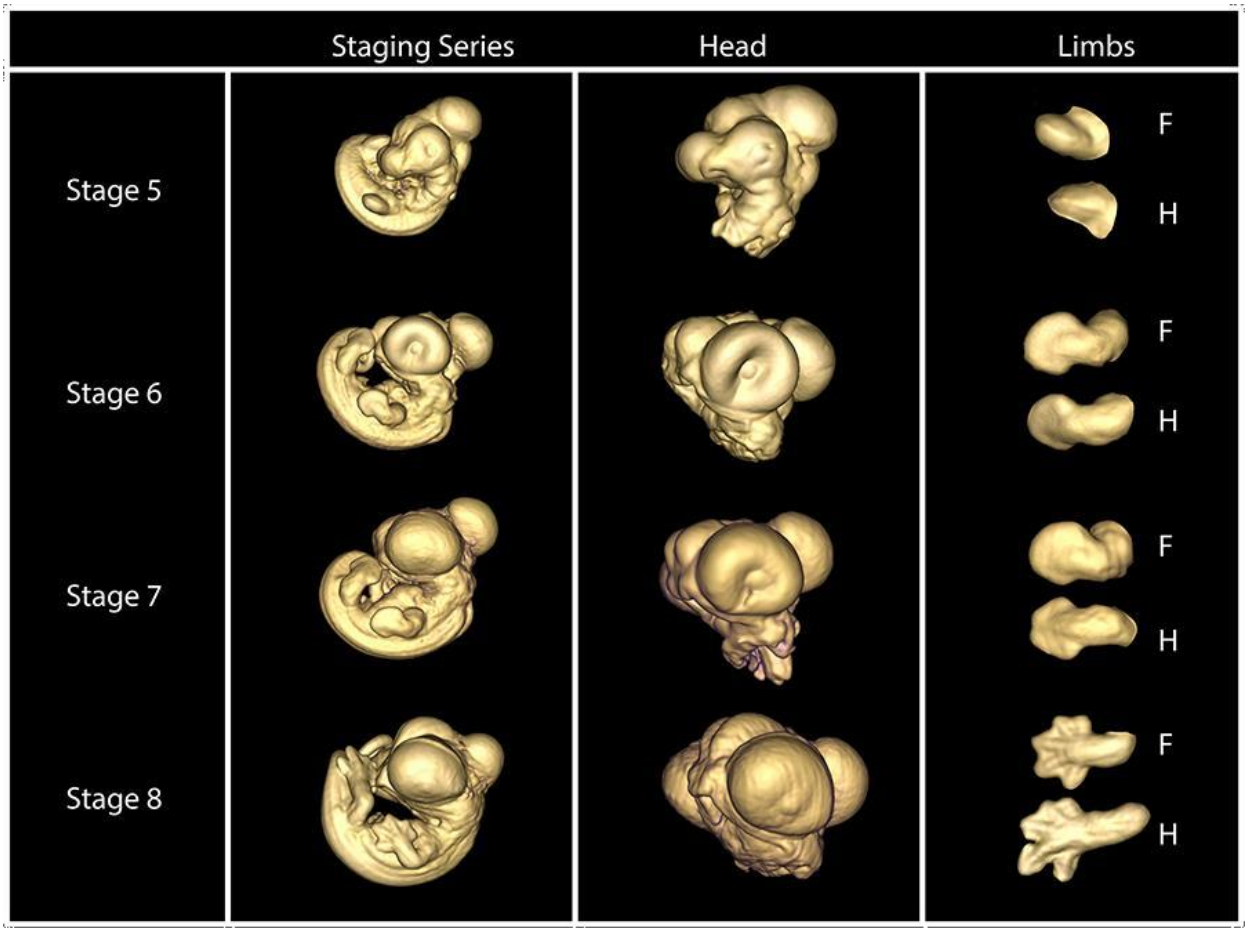

Figure 7. There-dimensional developmental staging series of *Anolis sagrei.* Developmental staging series for *Anolis sagrei.* Stage numbers are located to the left-hand column, aligning consecutively with each stage. See text for a full description of each stage. Stages later than Stage 15 cannot fit in the CT scanner as full embryos. H, hindlimb; F, forelimb.

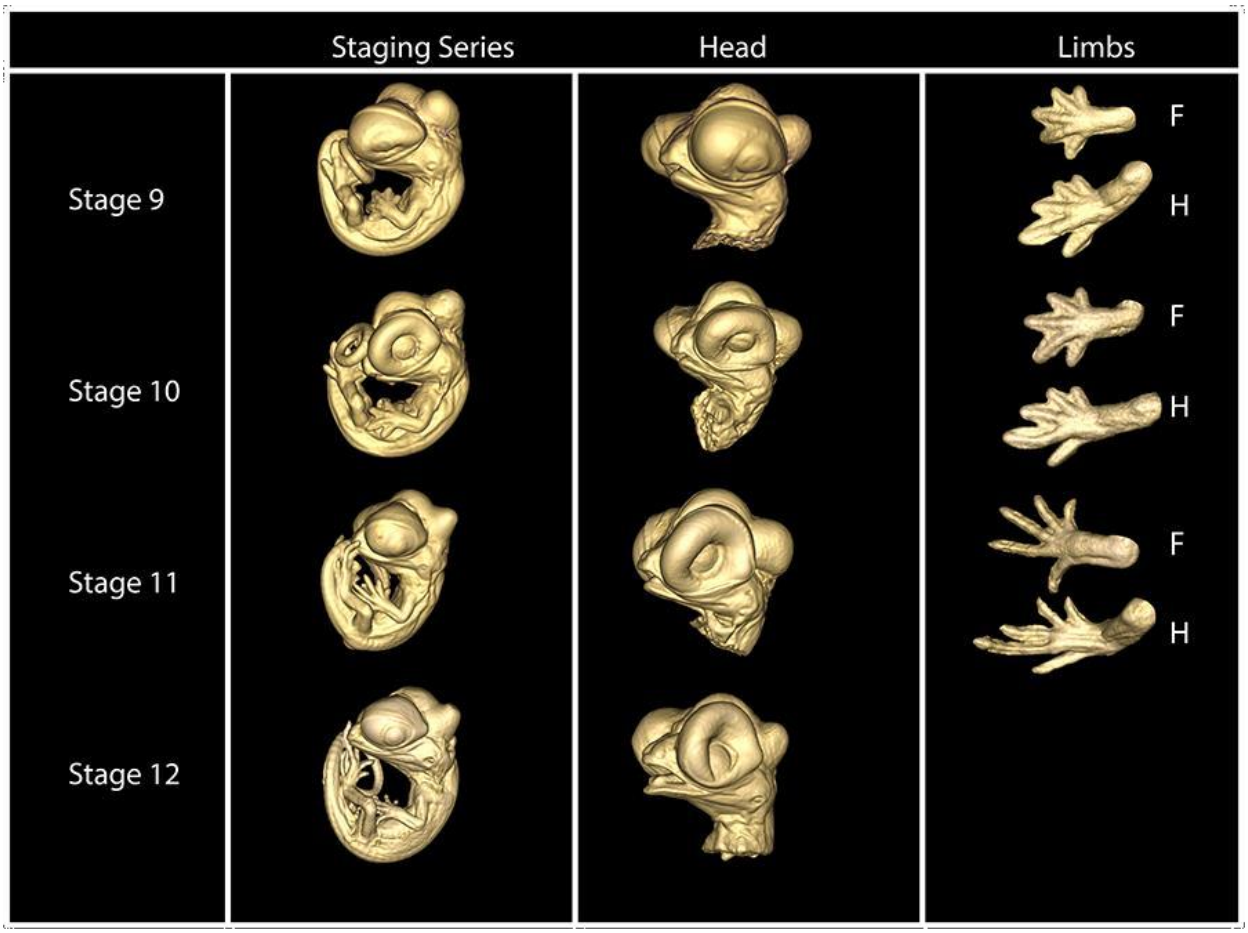

Figure 7. continued.

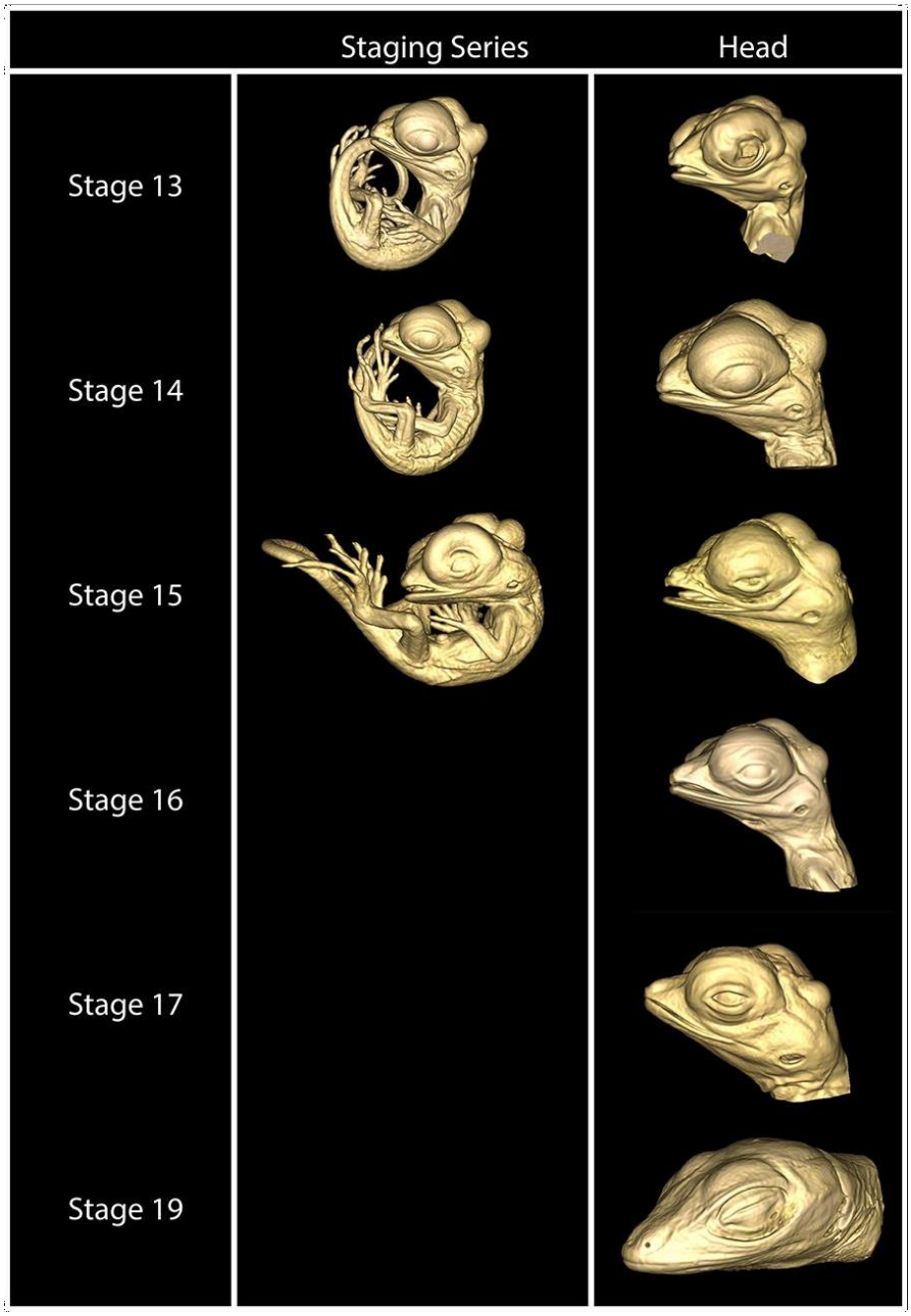

Figure 7. continued.

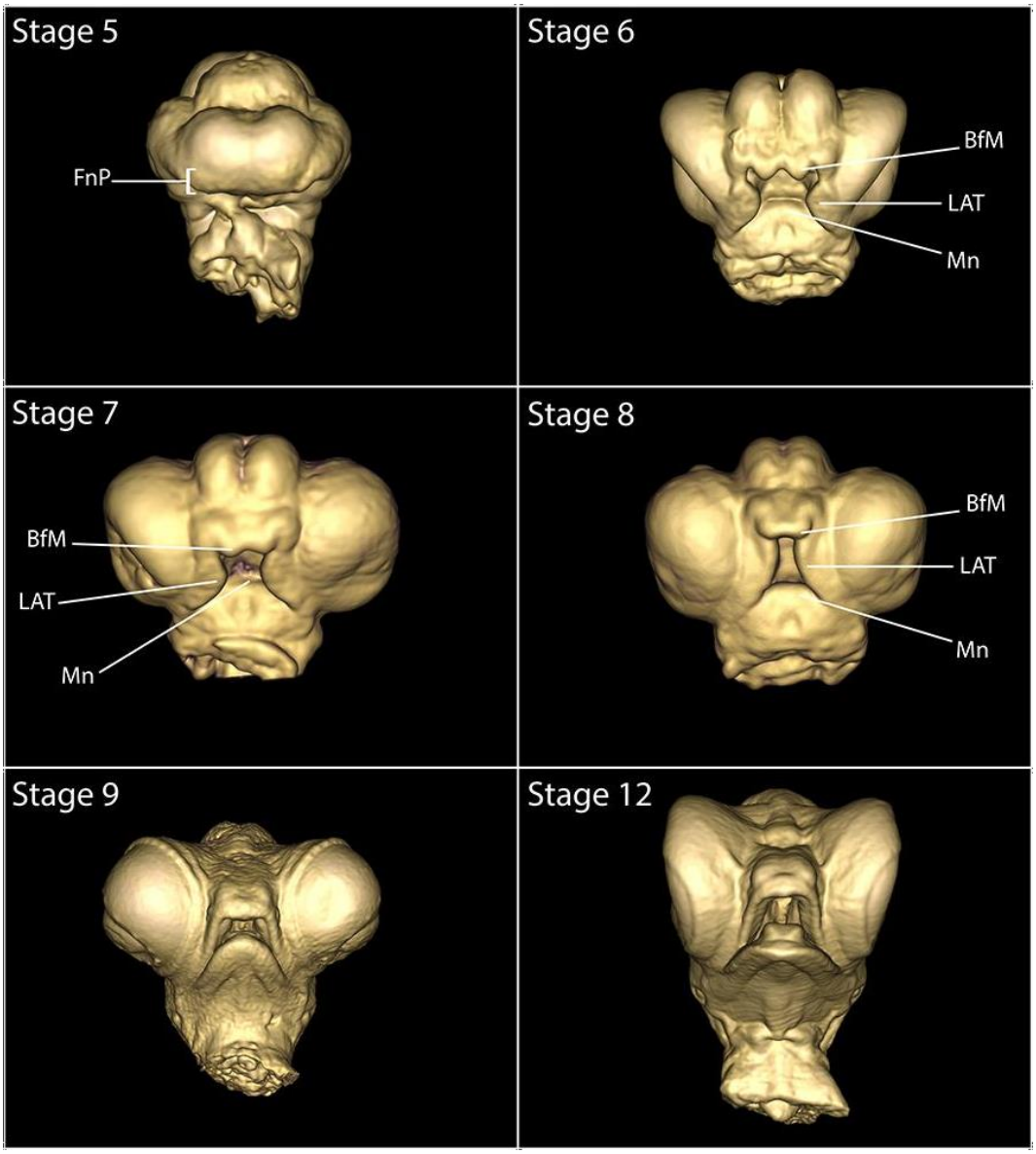

Figure 8. Volume renderings of prominent facial features. µCT volume renderings of prominent facial developments from different stages of development in *Anolis sagrei.* BfM, bifurcated midline; FnP, frontonasal mass; LAT, lateral; Mn, mandibular.

Brain

I performed a detailed study of brain development in *A. sagrei*. As a reference, I first describe the general shape and tissue composition of the adult *A. sagrei* brain, based on 3D rendering and segmentation of high resolution µCT scan data (Figure 9). Often, the five secondary vesicles of the embryonic neural tube are used to define the stages of brain development (Arey, 1974; Bellairs & Osmond, 2014; Senn, 1979; Griffing et al., 2019; Noro et al., 2009; Sanger et al., 2008; Wise et al., 2009). The five vesicles are the telencephalon, diencephalon, mesencephalon, metencephalon, and myelencephalon. Respectively, these give rise to the cerebral hemisphere, and olfactory region (telencephalon); epithalamus, thalamus, and hypothalamus (diencephalon); optic tectum and tegmentum (mesencephalon); tegmentum and cerebellum (metencephalon); and finally, medulla oblongata (myelencephalon) (Arey, 1974; Bellairs & Osmond, 2014; Senn, 1979; Griffing et al., 2019).

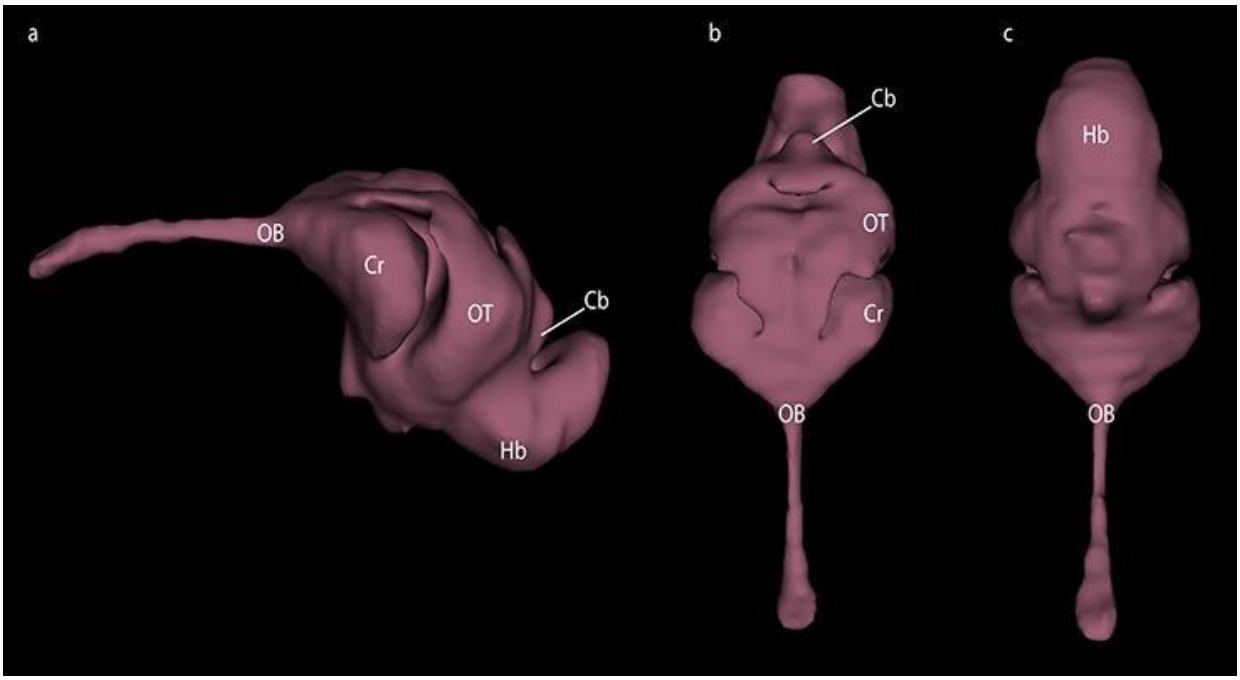

Figure 9. Three-dimensional rendering of adult brain. (a) Lateral, (b) dorsal and (c) ventral views of an Adult *Anolis sagrei* brain visualized through soft tissue µCT. Pictures are based on 3D volume renderings and segmentation of brains using 3D Slicer. Cb, cerebellum; Cr, cerebrum; Hb, Hindbrain; OB, olfactory bulbs; OT, optic tectum.

Stage 5: Developing cephalic bulges are distinct enough to distinguish into the cerebrum, optic tectum, and hindbrain.

Stage 6: The dorsal bulge that makes up the optic tectum is more exaggerated than in previous stage.

Stage 7: The cerebellum begins to form a more distinctive bulge caudo-ventrally.

Stage 8: Continued growth of the cerebrum and cerebellum.

Stage 9: The beginning of the olfactory bulb starts forming at the dorso-frontal position. Continued growth of the cerebrum and cerebellum.

Stage 10: Olfactory bulb has grown. The areas around the cerebrum and optic tectum are noticeably larger. Cerebellum and hindbrain have grown.

Stage 11: Regions of the brain, especially around the cerebellum and optic tectum, have increased in size compared to previous stage.

Stage 12: Cerebellum and optic tectum have increased in size again compared to previous stage.

Stage 13: Cerebellum and optic tectum are less distinct.

Stage 14: Optic tectum and cerebellum are less distinct.

Stage 15: Olfactory bulb has frown longer than in previous stage. Hindbrain has increased in size. Optic tectum and cerebellum are less distinct.

Stage 16: Optic tectum and cerebellum are less distinct.

Stages 17-19: No change from previous stage

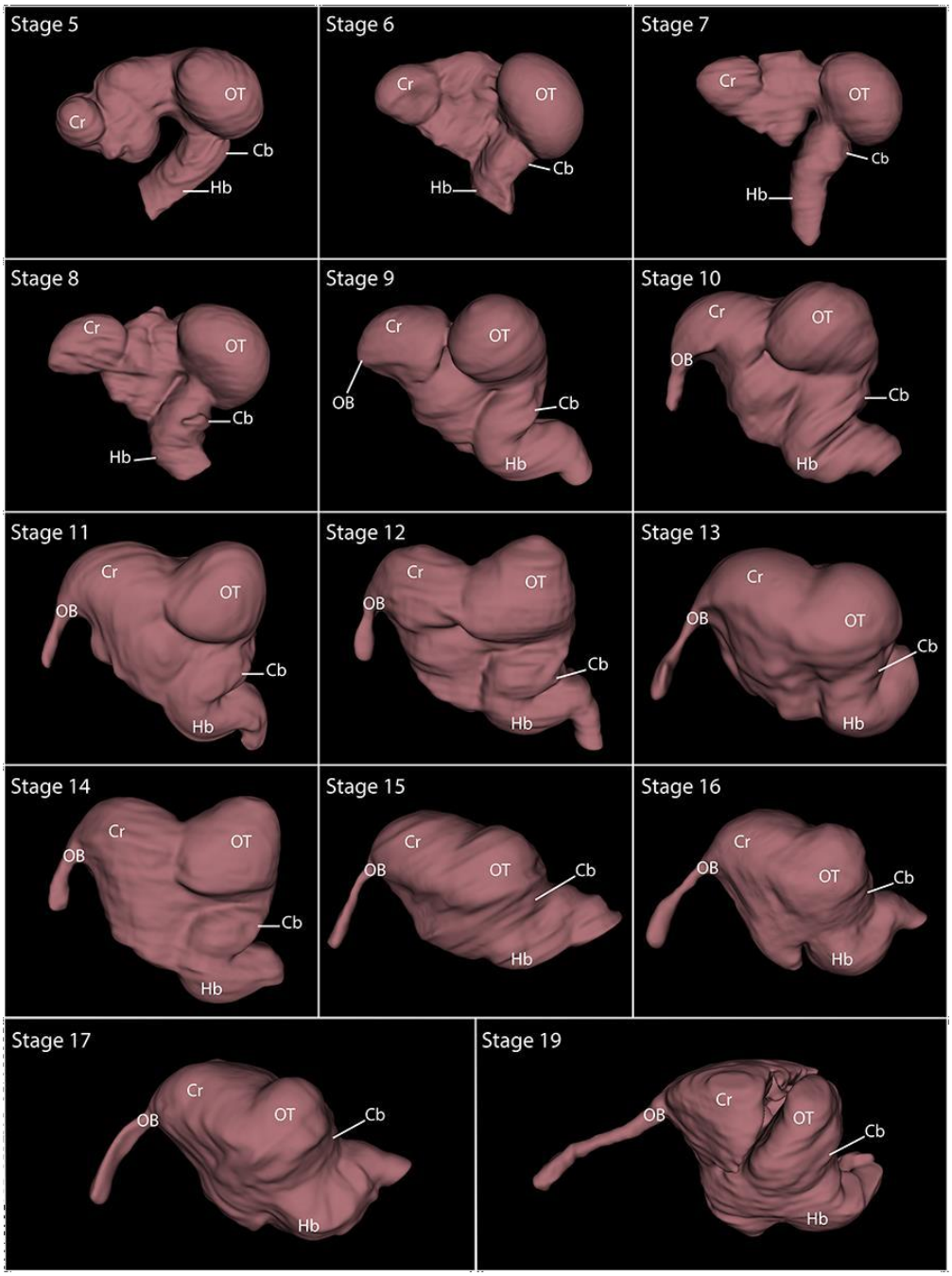

Figure 10. Three-dimensional rendering of embryonic brains. Lateral view of embryonic development of the *Anolis sagrei* brain visualized through soft tissue µCT. Pictures are based on 3D volume renderings and segmentation of brains using 3D Slicer. Cb, cerebellum; Cr, cerebrum; Hb, Hindbrain; OB, olfactory bulbs; OT, optic tectum.

Skull

I performed a detailed study of the skeletogenesis in *A. sagrei*, from onset of ossification to hatching. As a reference, I first describe the general shape and bone composition of the entire skull of the adult *A. sagrei*, based on 3D rendering and segmentation of high resolution µCT scan data (Figure 12). Based on the bone composition of the adult *A. sagrei* skull, I then mapped the skull ossification pattern and sequence of appearance of individual bones (Figure 13) of the entire skull, using high resolution µCT-scan data of developing skulls corresponding to different embryonic stages. Below I describe the ossification of the entire skull at each stage of embryonic development. Stages 1-11 did not have any visible ossification. Therefore, description of cranial ossification starts at stage 12 (Figure 7).

The general inspection of the adult skull of *A. sagrei* notes a slightly longer than wide skull. The snout is also relatively longer in comparison to other parts of the skull. The tooth bearing anterior tip of the snout, which includes the maxilla and premaxilla, stretched from there to the posterior end of the orbit. The orbital skull bones: the prefrontal, frontal, jugal and postorbital lie in the anterior half of the skull. The braincase in anoles does not include ossified elements at its anterior end and is surrounded by the jaw muscles laterally. The palate lies anterior-ventrally and laterally to the braincase.

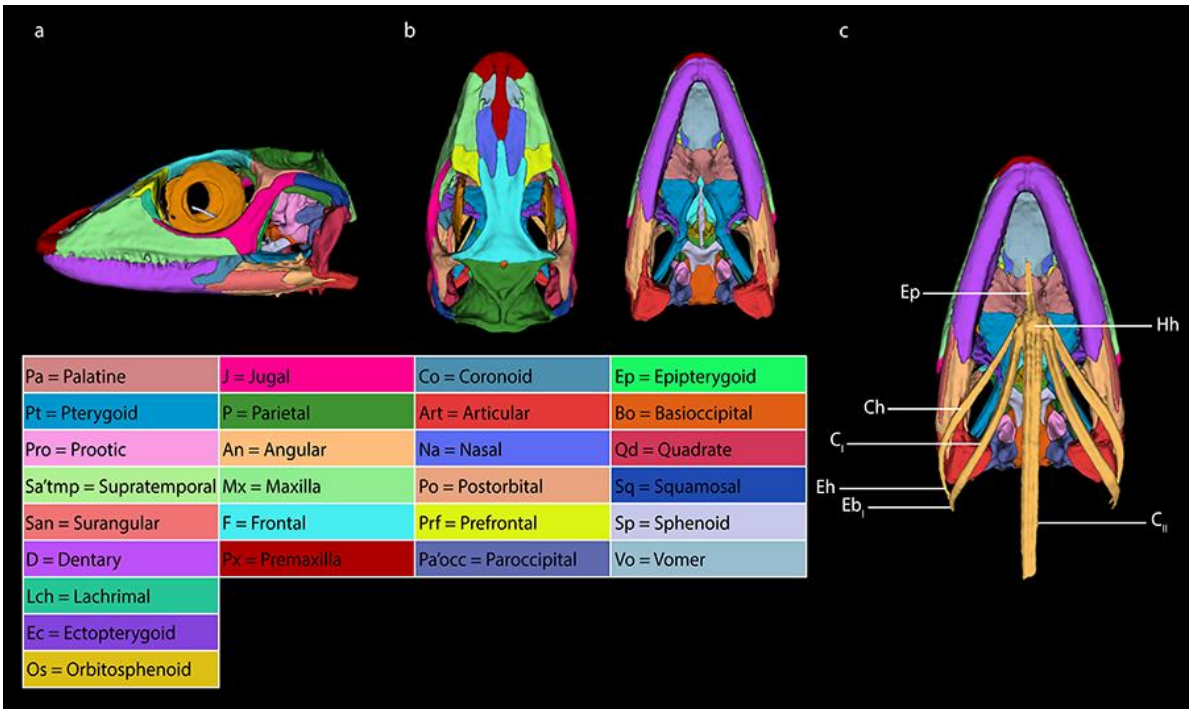

Figure 11. Three-dimensional rendering of mature, adult skull. Adult anatomy of the *Anolis sagrei* skull. Lateral, dorsal, and ventral views of the skull of *Anolis sagrei*. The hyoid apparatus has been removed in the ventral view (b) to allow for better visualization of the palate. The hyoid can be seen illustrated to the far right (c). Pictures are based on 3D renderings and segmentation in 3D Slicer of individual bones with different colors (see color coding in table). Ep, entoglossal process; Hh, hypohyal; Ch, ceratohyal; C_I, ceratobrachial I; C_{II}, ceratobrachial II; Eh, epihyal; Eb_I, epibranchial.

Stage 12: The palatine, pterygoid and prootic are first visible ossification centers to form. The palatine is located anteriorly to the pterygoid. The pterygoid forms the posterior-most part of the palate. The prootic, an irregularly shaped bone, forms the lateral sides of the braincase.

Stage 13: Ossification of many bones associated with the circumorbital, temporal, and braincase begins. First visible as a triangularly shaped bone right above the dentary, the premaxilla, located at the anterior front of the snout, and posteriorly to the nasal bone. The maxilla is a large surface bone that makes up the lateral-anterior walls of the orbit of the eye. Framed anteriorly by the maxilla and posteriorly by the postorbital, the jugal begins to ossify, as a large, curved bone that contributes to the lateral part of the orbit. The parietal, seen as two slender angled slivers of bones at this stage, has begun to cover the dorsal posterior portion of the skull. Frontal ossification is seen as a narrow midline that is located dorsally above the palate bones and is coming in contact with posteriorly with the parietal. An irregularly oval shaped bone at this stage, the supratemporal, is located posteriorly at the end of the braincase. It is located to the parietal dorsal laterally. The dentary, a large boomerang shaped bone that starts ossifying at the anterior portion near the snout, and laterally underneath the maxilla and jugal bones, is also coming into contact with the surangular posteriorly and the coronoid dorsal-laterally. The surangular and angular have begun to connect and are located posterior-laterally.

Stage 14: Ossification of circumorbital, skull roof, temporal, braincase, and mandible continues. The nasal bones are irregularly shaped bones that are located anteriorly to the premaxilla, and posteriorly to the prefrontal and frontal circumorbital regions. The maxilla has begun to connect to the jugal. The prefrontal connects posteriorly to the frontal. Another orbital bone, the

postorbital bone is a triangular bone that is situated dorsally right above the jugal and anterior-laterally from the squamosum. It also ventrally located under the frontal and parietal. Following the postorbital, the squamosal bone is a curved bone that has begun to connect to the jugal and postorbital anterior- laterally and is connected to the paraoccipital posteriorly. Inside the skull, the palatine has started to connect with the pterygoid and the epipterygoid has appeared as a long and slender bone that is situated ventrally to the pterygoid. The quadrate, a laterally winged shaped bone is positioned ventral-dorsally to the articular, and laterally to the paroccipital. The dentary has begun to fuse with the coronoid and angular. Making up part of the posterior part of the braincase, the paraoccipital has begun to ossify and is located anteriorly to the prootic and the parietal dorsally.

Stage 15: Ossification of the vomer begins here. It is a thin triangular bone, located anterior-ventrally under the premaxilla, laterally to the maxilla, and posteriorly to the palatine. Continued fusion and ossification of jugal, maxilla and prefrontal bones observed. Frontal and parietal bones have connected. Moving to the orbital bones, the lacrimal makes its appearance as part of the orbital surface, connecting anteriorly to the maxilla and prefrontal and posterior-laterally to the jugal. The squamosal and supratemporal have connected. The sphenoid and basioccipital ventrally attached to one another, marks the beginning of ossification of the braincase floor. Continued ossification and fusion of bones observed.

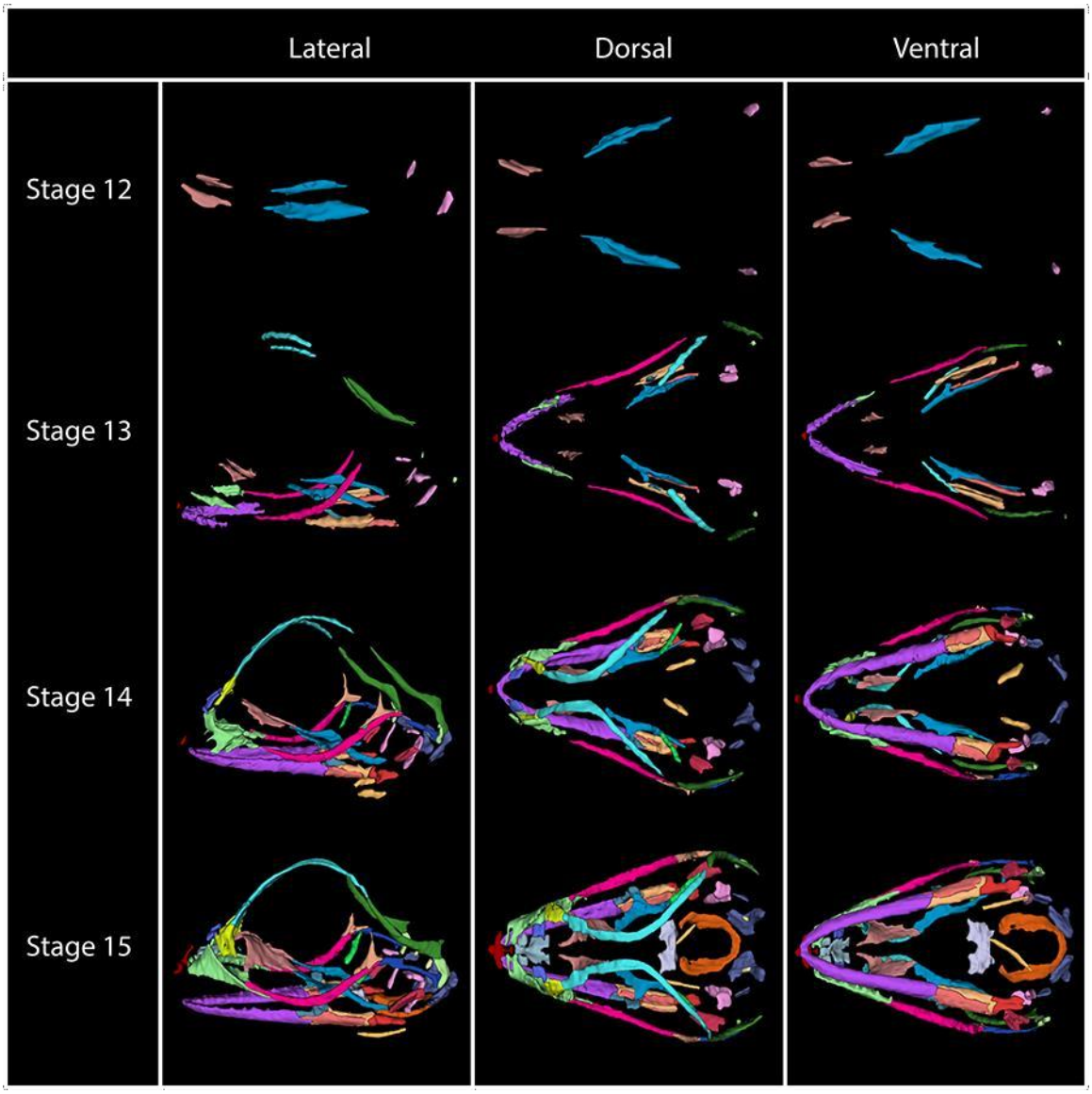

Figure 12. Three-dimensional rendering illustrating progression of skull formation. Embryonic development of skull bones in *Anolis sagrei.* Stage numbers are located to the left-hand column, aligning consecutively with each stage. Views of different developing skull stages in *Anolis sagrei* have been split into three different columns: Lateral, dorsal and ventral. Pictures are based on 3D volume renderings and segmentation of individual bones using 3D Slicer with different colors (see color coding in Figure 11).

Stage 16-18: The orbitosphenoid, a boomerang shaped bone, hovers vertically in the middle of the skull, underneath the frontal and parietal, anteriorly to the paraoccipital and prootic. It does not come in contact with any bones. Palatine and vomer have connected. In addition, the ectopterygoid begins to ossify, an irregularly shaped bone which connects laterally to the pterygoid and medially to the dentary and coronoid. Paraoccipital and prootic have connected.

Stage 19: Appearance of stapes observed, short horn shaped bones that lie on the posterior-laterally sides of the braincase. Eventually disappears during maturity. All bones have connected, and ossification complete in most bones. The parietal bone eventually ossifies to cover hole after hatching and before maturity.

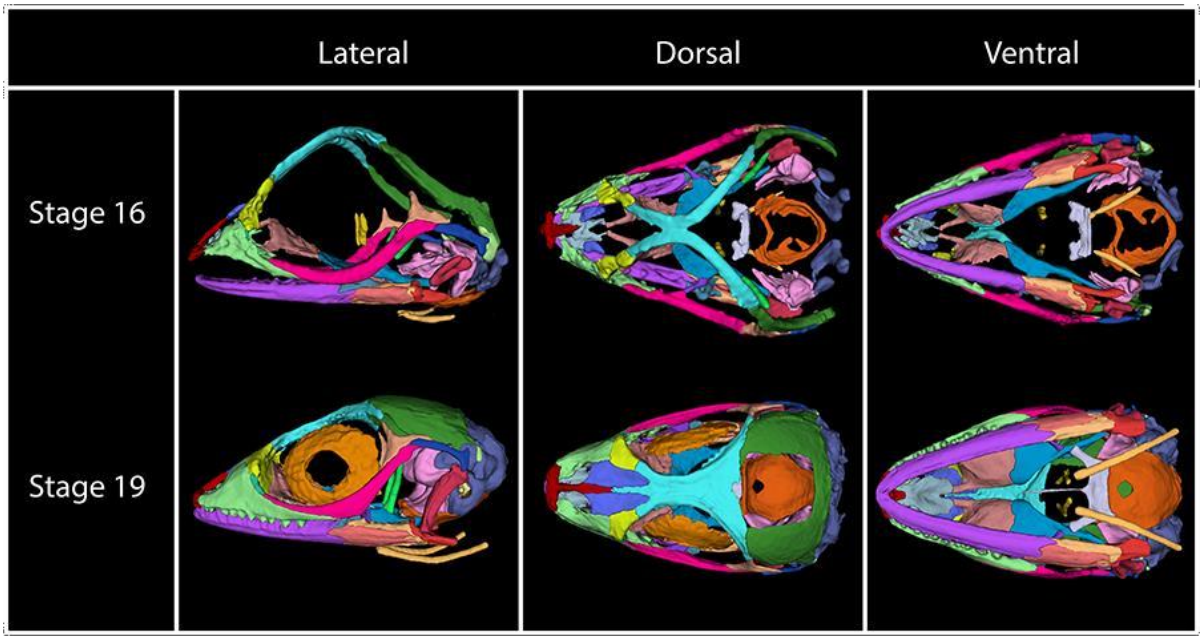

Figure 12. continued.

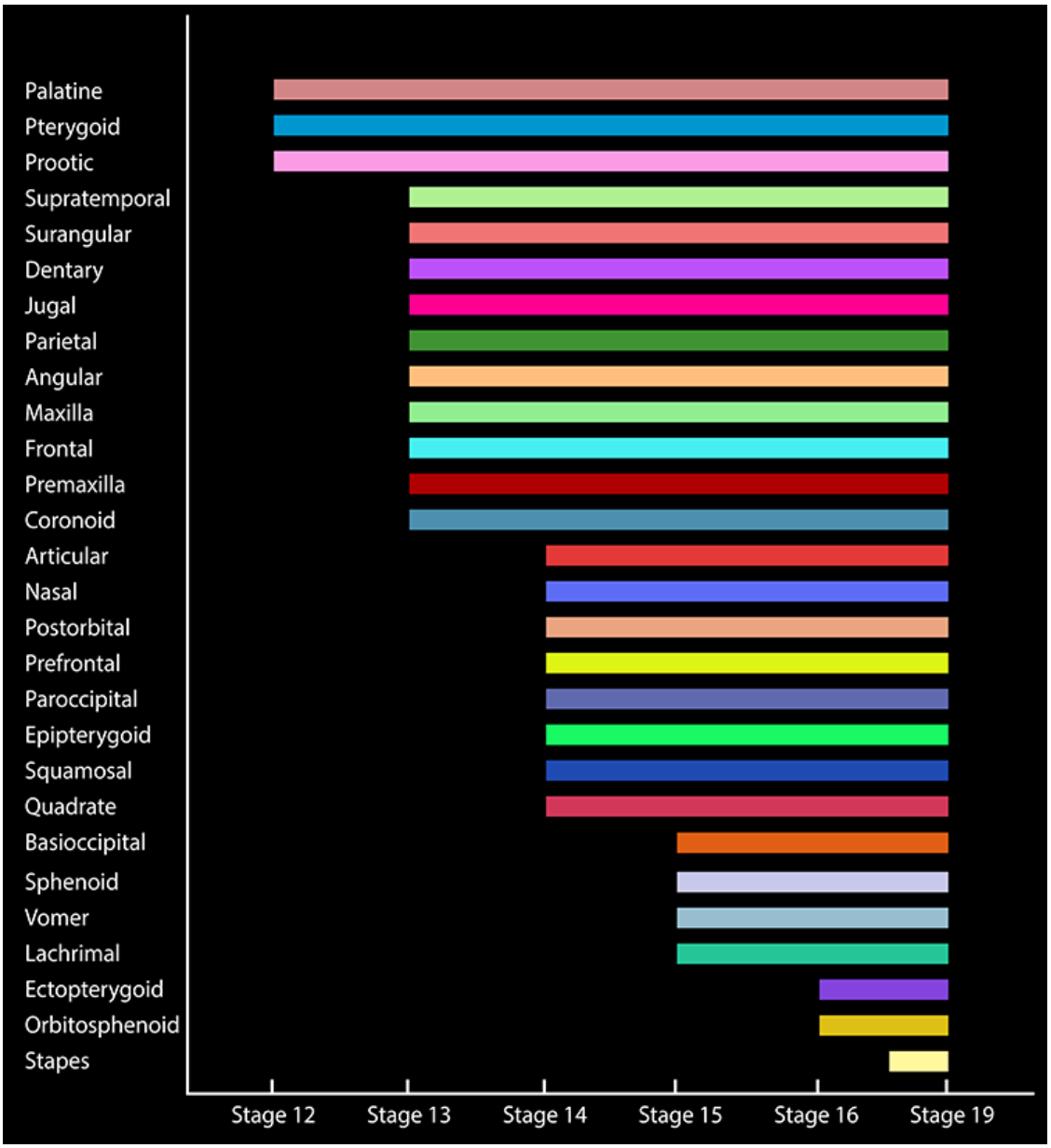

Figure 13. Ossification sequence of skull bones. Ossification sequence of skull bones in *Anolis sagrei.* The presence of individual skull bones at different developmental stages indicated in stage # on the horizontal X axis. Bones are in order according to when they first appear at each stage, indicated on the vertical Y axis. Color coding on horizontal bars is based on color coding seen in Figure 11.

CHAPTER 4

EDUCATIONAL EXERCISE

Anolis Embryo and Skull Development

Knowledge of embryonic development is essential to understanding the morphological diversity and the evolution of development among vertebrates. Biology students often struggle to interpret three-dimensionality of an embryo from textbooks that rely on static, 2-dimensional (2D) schematics (Chekrouni et al., 2020). This is particularly true for the dynamic progression of morphogenesis, as each organ system differentiates and grows along multiple dimensions. To overcome these challenges, 3D digital models can be used along with the traditional 2D schematics. 3D models can be manipulated by students to see developing structures with regards to age, developmental age, and impact of disease or injury (Backhouse et al., 2017; Fredieu et al., 2015). Previous studies to facilitate embryology education on an understandable level using 3D models has shown to add educational value and improve student learning experience (Chekrouni et al., 2020; Garas et al., 2018; Kazoka et al., 2021; Prange-Kiel et al., 2016). This assignment will incorporate interactive 3D visualization technology with the more classical educational methods of 2D schematics to provide students with an opportunity to use 3D models in their education, synthesizing an understanding of vertebrate embryogenesis.

For that, a 3D atlas of *Anolis sagrei* embryology was created, encompassing over 60 interactive 3D-models encompassing the range of embryonic development. The learning

activity to go along with these interactive 3D models aims to enhance embryology education at a level appropriate for early undergraduate students. The exercise will review development of the body, limb, head and skull development. Although the assignment was developed with undergraduate students in mind, it may also be used in high school classrooms for juniors and seniors. Following this exercise, students should be able to apply what they have learned to the development of other animals, particularly developmental model systems (I.e., chickens and mice) and human development.

Learning outcomes (objectives)

- Become familiar with the embryonic stages of development.
- Become familiar with vocabulary of embryological and skeletal anatomy
- Recognize key morphological aspects of different stages of development (e.g., craniofacial, fore and hind limb)
- Applying this knowledge to other species (i.e. human development).

Anticipated time

1.5 hours.

Materials

www.anolisevodevo.space – website that will host the assignments and embedded Sketchfab 3D models of embryological and skeletal development. 3d prints of full body, and heads of embryos: 25 in total– accompanies the embryological portion of the assignment, used for studying the different stages of development.

Full Embryo

Learning strategy

Embryo models will be posted online at www.anolisevodevo.space. 3D printed models will be provided to the classroom, allowing students to not only see a 3D embryo, but also to touch it without the fear of damage or the need to purchase expensive microscopes. 3D models are also expanded 10X their original size, providing greater opportunity to observe fine details. In the first assignment the goal is to align the 3D models in chronological order. Students will be asked to provide the characters used to generate the order. In addition to this, students will have to draw out the stages and label key structures. Once completed, the correct answers can be reviewed on www.anolisevodevo.space via a password protected page.

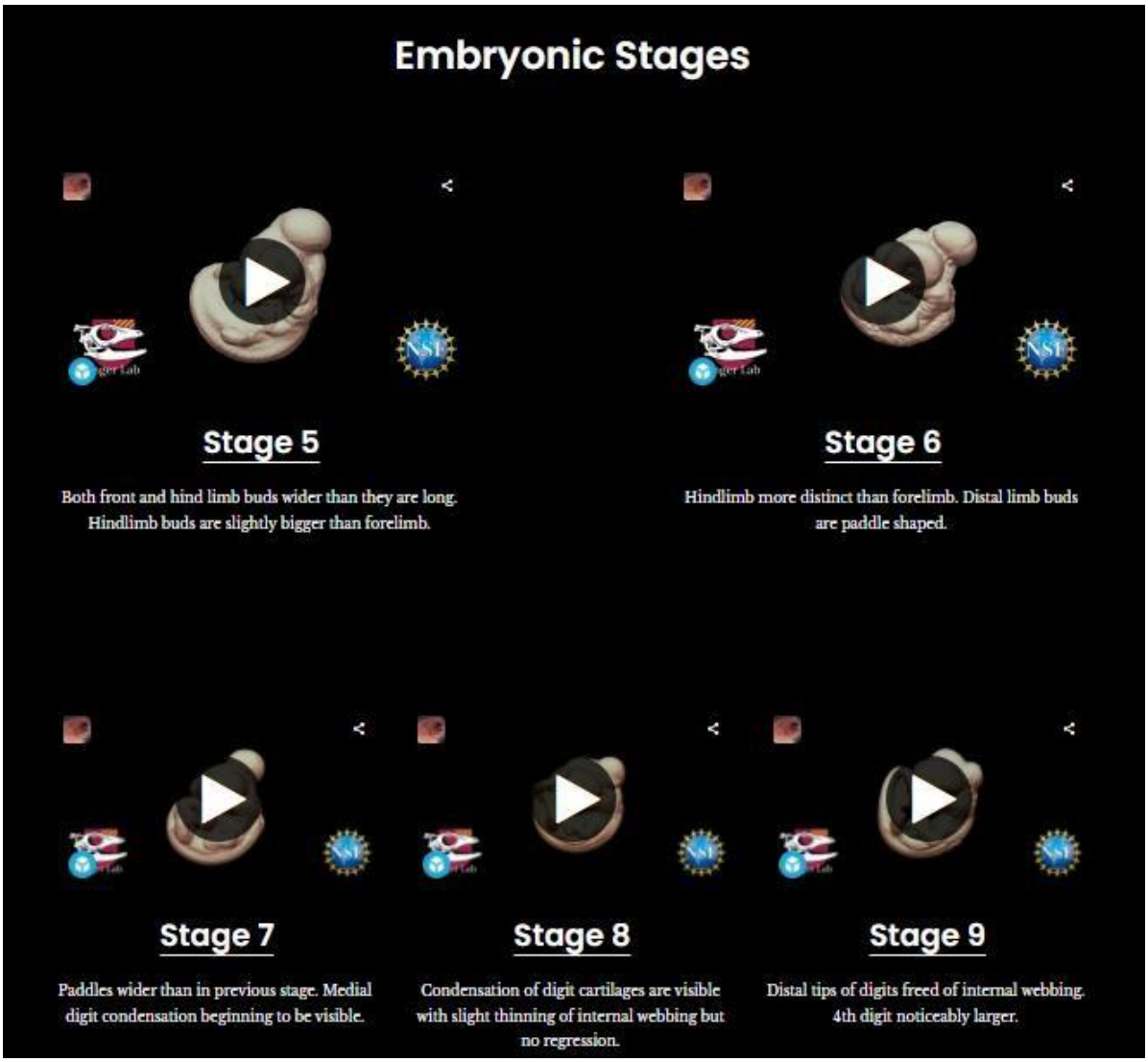

Figure 14. 3D embryo models on www.anolisevodevo.space. The anolisevodevo.space webspace (above) holds the embryonic full body stage 3D models which can be fully manipulated.

Example:

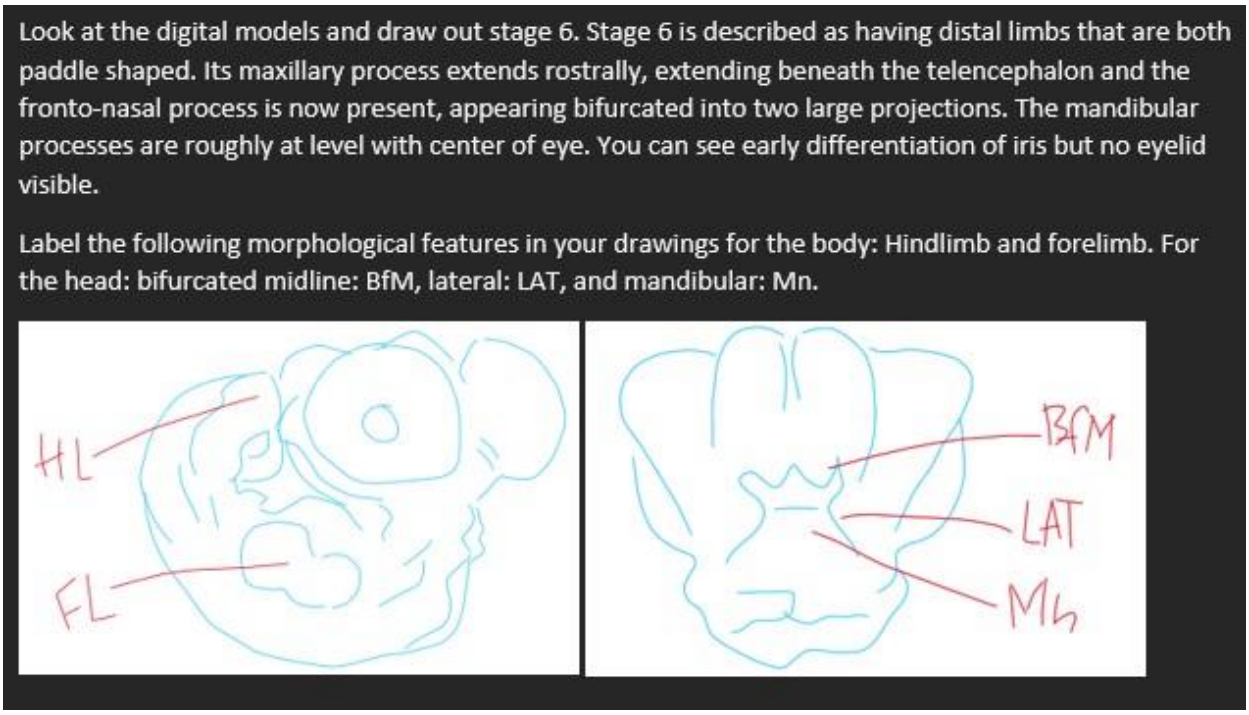

Figure 15. Body and face example question. Body and Face example question and the answer to the assignment the students will work on.

Questions:

In this exercise you are looking at 3D prints of whole, intact lizard embryos at different stages of development. The embryonic period of development is divided into specific stages based on changes that occur during development. The embryonic period of *Anolis sagrei* is divided into 19 stages of development. You will be looking at 14 of those stages, starting with stage 5. Look at the 3D models, observe key morphological traits from one stage to another and align them in order of chronological development. Provide a rationale on the order you choose. What characters are changing?

1. Draw out changes in limb and head development in their appropriate chronological order. Label forelimb, hindlimb, fore-, mid- and hindbrain. Also label the major body axes: the anterior, posterior, ventral and dorsal axis. Write 1-2 sentences of what embryological changes you observe along stages 5-12.
2. Once you've completed drawing, labeling, and aligning the stages in their chronological order, go to www.anolisevodevo.space to check your answers. Make corrections where necessary.

Face

The ability to look at the facial morphogenesis of embryos without bodily obstructions allows for a close-up inspection of the eye, and snout formation. The main goal for this second part of the assignment, much like above, is to align the 3D models in chronological order and provide descriptions of the characters used to determine that order. Virtual models of the head will be posted online via www.anolisevodevo.space and 3D

printed models of heads will be provided to the classroom. The goal of this assignment is to gain a better understanding of key facial processes that develop during embryogenesis and to become familiar with facial morphology (such as the bifurcated midline, mandible, etc.).

Questions

In this exercise you are looking at 3D prints of the embryonic heads at different stages of development. Much like in the previous exercise, look at the 3D models, observe key morphological traits from one stage to another. Notice the morphological development of the frontonasal mass, the mandible, the maxillary process etc., and align the heads in chronological order of development starting with stage 5.

1. Draw out the stages in their appropriate chronological order. For stages 6-8 prominent facial morphogenesis occurs along the bifurcated midline (BfM), lateral (LAT), mandibular (Mn); label them appropriately. Also label the anterior, posterior, ventral and dorsal axis; and write 1-2 sentences of what ontogenetic changes you are observing in each stage.
2. Once you've completed drawing, labeling, and aligning the stages in their chronological order, go to www.anolisevodevo.space to check your answers.

Skull

The skull develops as a disconnected series of ossification centers. Therefore, the developing skull cannot be 3D printed. Instead, this exercise will rely on interactive 3D models maintained on www.anolisevodevo.space. This activity provides digital models of the developing skull morphology of *A. sagrei*. Because many people have some familiarity with the skull, this portion of the assignment will use the adult skull as a reference. On the www.anolisevodevo.space website the adult skull will be provided with a key to the bones that can be used to identify the bones in earlier stages.

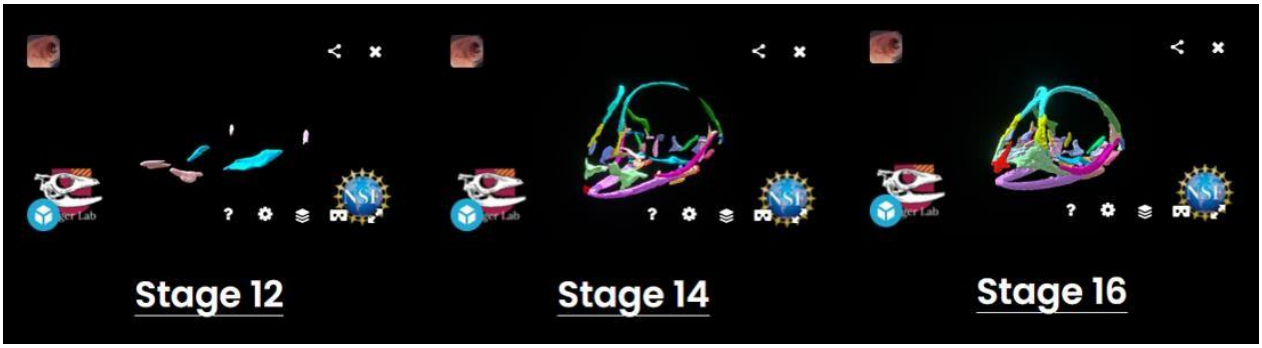

Figure 16. Ossification sequence on www. anolisevodevo.space. Early, middle, and late stages of ossification in *A. sagrei* embryos. These models are posted on www. anolisevodevo.space.

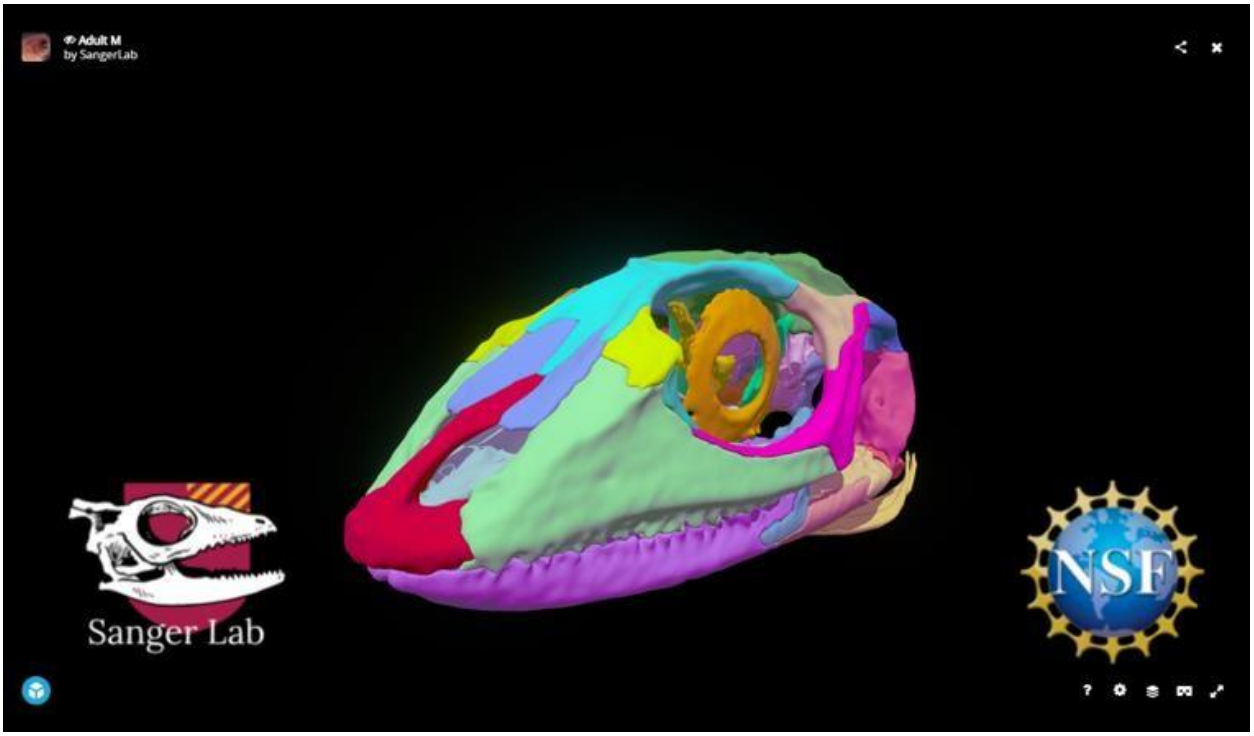

Figure 17. Adult skull on www.anolisevodevo.space. Adult *A. sagrei* skull model posted on www.anolisevodevo.space.

Starting with the adult skull: draw the skull and label the bones appropriately while using the 3D models and list of abbreviations as a reference. Pay attention to the placement of ossification centers (i.e., between two bones, at the very anterior portion, making up some bigger part of the orbital, snout, dentary, or braincase region, etc.). Make sure to label the anterior, posterior, ventral and dorsal axis of each stage. At the end of the assignment, another link on the www.anolisevodevo.space page will provide the correct chronological order of the skull staging series. The main goal with this lesson is to learn bone vocabulary, bone placement, and symmetry.

Example:

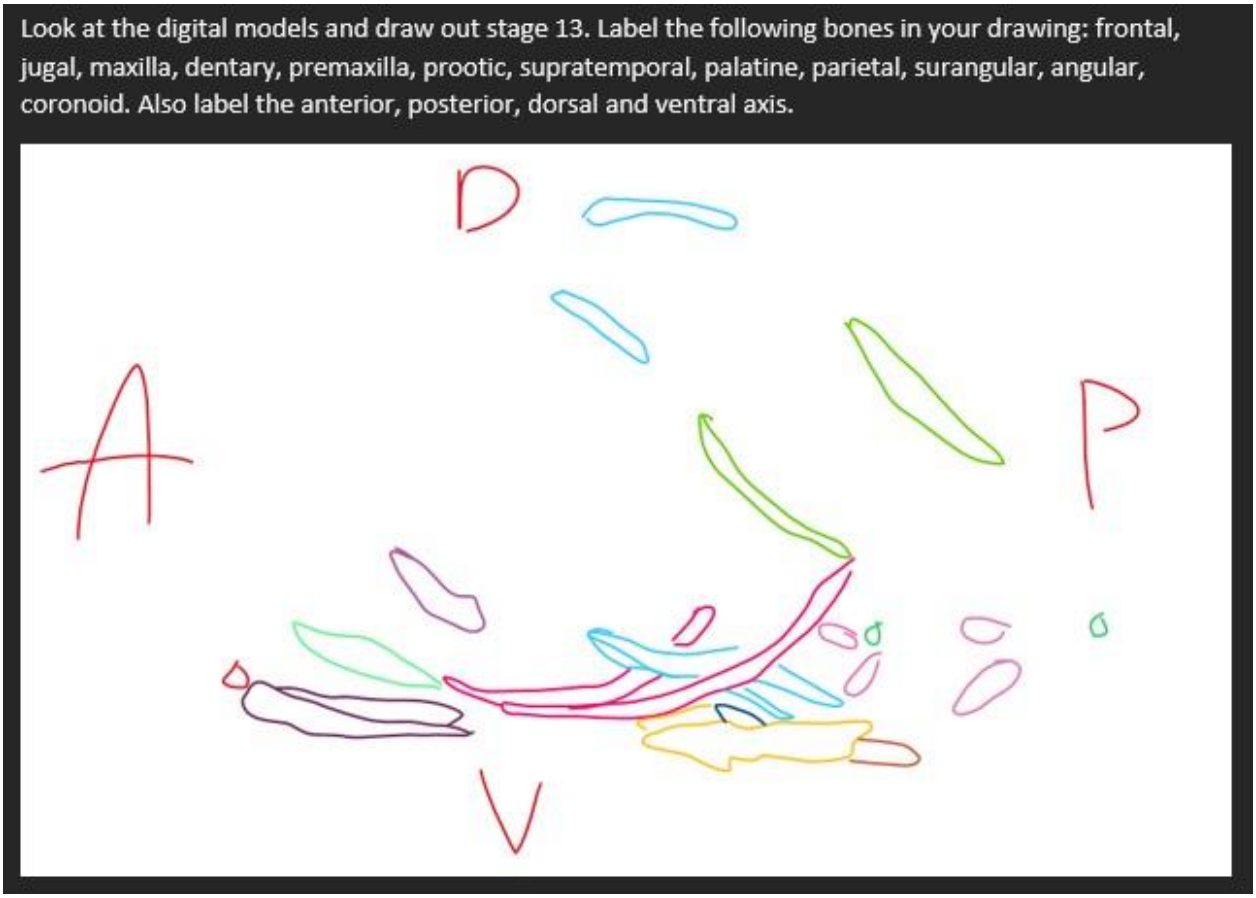

Figure 18. Body and face example question. Skull assignment example question and answer that the students will work on.

Questions

1. What are the first bones that form?
2. What bones appear at stage 14 that are not in stage 13?
3. What bones make up the snout? Surround the orbit? The lower jaw? The snout?
4. Compare the adult skull to the hatchling skull. What bones are not fully formed at hatching?
5. At what stage does the frontal connect to the prefrontal bone? The prootic to the paroccipital? The maxilla to the premaxilla? The pterygoid to the palatine?

List of Abbreviation

- **Embryo:**
    - BfM: bifurcated midline
    - FnP: fronto-nasal mass
    - LAT: Lateral
    - Mn: mandibular
    - F: forelimb
    - H: hindlimb
- **Skeleton:**
    - Pa: Palatine
    - J: Jugal
    - Co: Coronoid
    - Ep: Epipterygoid

- Pt: Pterygoid
- P: Parietal
- Art: Articular
- Bo: Basioccipital
- Pro: Prootic
- An: Angular
- Na: Nasal
- Qd: Quadrate
- Sa’tmp: Supratemporal
- Mx: Maxilla
- Po: Postorbital
- Sq: Squamosal
- San: Surangular
- F: Frontal
- Prf: Prefrontal
- Sp: Sphenoid
- D: Dentiary
- Px: Premaxilla
- Pa’occ: Paroccipital
- Vo: Vomer
- Lch: Lachrimal
- Ec: Ectopterygoid
- Os: Orbitosphenoid

Glossary

Stage - sequence of ontogenetic changes during embryonic development

Anterior - front

Posterior - back

Medial - midline

Lateral - side

Dorsal - top

Ventra - bottom

Rostral – toward the front (head)

Caudal - toward the end (bottom)

Alternative learning strategy for Bodies and Heads

If 3D prints are not available to the class, the second option is to access the 3D models online via www.anolisevodevo.space to complete the assignment. On the www.anolisevodevo.space page the models will be randomly assorted. In the document mentioned in previous assignments for Body and Face, students will draw out and label the stages of development and use their drawings to place the models in their correct chronological development. Students will also be adding 1-2 sentence descriptions of what morphological development they observe in the 3D models. Once finished drawing the

models and completed the staging, a second link will be provided with the correct staging series.

Assessment method

An in-class activity that is meant to be used to have a hands-on learning experience in a group where students can discuss and think off each other to complete the assignment. The assignment will be graded based off of completion of questions.

CHAPTER 5

DISCUSSION

I present here a staging series for the post-ovipositional development of *Anolis sagrei.* My study advances a previous 2D staging series based on light microscopy (Sanger, Losos, et al., 2008). Prior to this study, several developmental staging series have been published for squamates (Boback et al., 2012; Boughner et al., 2007; Griffing et al., 2019). To date, few staging series have implemented non- destructive µCT techniques and contrast enhanced µCT. Following from Sanger et al. (2008), my study describes coarse features of the entire body that may help an investigator stage an embryo of *A. sagrei*, embryos from experimental treatments, or those from closely related species. However, I report the details of craniofacial development, including the face, skeleton, and brain, using CT-scanning and 3D segmentation to provide detailed models.

Anolis as a Developmental Model

There still is not a single taxon of lizard that has been adopted among as the developmental model to study, but many have been proposed (Griffing et al., 2019; Ollonen et al., 2018; Sanger, et al., 2008; Wise et al., 2009). *Anolis* lizards are a long-used model is studies of ecology, evolution, and behavior with over 27,000 articles currently published on anole research since 1980 (Losos, 1994; Losos & Schneider, 2009a; Sanger, 2012). More recently, studies in dimorphism both across species and between sexes looking into limb length variation based on habitat specific capabilities or sexual divergence in craniofacial

growth has expanded those fields (Sanger et al., 2012, 2013; Sanger & Kircher, 2017). With the breadth of work on anoles just continuing to expand, anoles are becoming one of the most widely studied model systems in various fields, including those examining developmental and molecular processes underlying lineage diversification and extreme morphologies (Alföldi et al., 2011; Rasys et al., 2019; Sanger et al., 2018; Sanger & Kircher, 2017). Following the publication of the *A. carolinensis*, green anole, genome, anoles can be argued to have been the first squamate species with the ability for being developed for experimental embryological studies and development, and functional genomics (Alföldi et al., 2011; Sanger & Kircher, 2017). This includes studies within species, among closely related anole species, and serving as a representative squamate for comparisons among distantly related amniotes.

Anolis is a well-established example of adaptive radiation, specifically the anoles occupying the islands of the Greater Antilles (Losos et al., 1998; Losos & Schneider, 2009b; Williams, 1983). Their repeated evolution has offered the opportunity to test many generalizations about evolutionary processes. Because of this, anoles have become one of the most widely studied models for the relationship between ecology and morphological diversification (Losos & Schneider, 2009a; Muñoz et al., 2014; Sanger et al., 2018). With this in mind, anoles has expanded into more recent areas of interest, such as obtaining an understanding of how anole development factors into adaptive radiation. Anoles have been previously studied in terms of adaptive radiation, for their rapid accumulation of lineages and different phenotypic evolutions (Losos & Ricklefs, 2009; Stroud & Losos, 2016). This has more recently expanded into more specific research in terms of development, such as

the research into adaptive radiation between species possessing similar limb morphologies that have converged to have similar alternations to their growth trajectories (Sanger, Revell, et al., 2012). It has also reached to include studies of development of toe-pads among genus's using developmental data to derive a potential developmental constraint in the evolution of digits and tails (Griffing et al., 2021).

Researchers interested in the evolution of amniotes drawn from comparisons among the amniote clades, especially birds and mammals have been integrating the morphologically diverse anoles, which follow unique patterns of ecomorphological convergence (Sanger et al., 2012). As the utility of anoles has grown, they have been used for comparisons among distantly related amniote lineages in studies including studies of heart development (Jensen et al., 2013; Koshiba-Takeuchi et al., 2009), tail regeneration (Hutchins et al., 2014, 2016; Ritzman et al., 2012), longitudinal body axis formation (Eckalbar et al., 2012; Kusumi et al., 2013), external genital (i.e., phallus) development (Gredler et al., 2014, 2015; Infante et al., 2015; Tschopp et al., 2014) and new tissue and ex-ovo embryo culturing techniques (Diaz & Trainor, 2015; Park et al., 2014; Sanger & Kircher, 2017; Tschopp et al., 2014). Incorporation of anoles in studies will elucidate more developmental peculiarities of amniote development with greater resolution than previous comparisons among classic model species alone (Sanger, 2012, 2021; Sanger et al., 2012, 2013b).

Anoles have provided a benchmark for researchers interested in craniofacial development (Sanger et al., 2012, 2013, 2021), which is why I have invested in detailed descriptions of the anole head herein. Anoles are a highly diversified species that have

converged on similar craniofacial morphologies with both intra- and inter- specific patterns of divergence reflecting their adaptations to different portions of their habitats (Sanger et al., 2012, 2013). Because of this, many studies have come forth regarding their craniofacial development, such as studies in relation to their craniofacial sexual dimorphism regarding sex-specific variation wherein males are typically larger in most morphological aspects. Other studies include developmental experiments, especially regarding the formation of the craniofacial morphology of embryos during development. These embryos are especially susceptible to increasing temperatures during development, specifically in craniofacial development which can cause morphological abnormalities in the facial structure during development (Sanger et al., 2018, 2021). With this in mind, my work indicates the developmental shifts that occur during both early development and ossification of craniofacial tissue. Furthermore, these changes transfer to the conserved adult skull shapes and the common bone features observed among anole lizards, further heterochronic studies comparing anole species can be done.

CT Scanning

I integrated micro-CT-scanning and tissue segmentation to create inteactive3D models complimentary to the staging series to Sanger et. al. 2008 (Sanger, et al., 2008)**.** The CT- scanning process was done separately for both soft tissue and mineralized tissue. These tissue- stained specimen were then scanned to capture DICOM stacks of the body and face. Once completed, the DICOM stacks were pulled into 3D Slicer, a free CT scan segmentation program, used for rendering 3D models out of CT scans and segmenting out certain parts of anatomy**,** such as the brain in this case. Brains were segmented from

different stages and the scans were rendered into 3D models. These models would then be uploaded onto Sketchfab, a free 3D model uploading website.

CT-scanning has recently become an attractive option for analyzing morphological phenotypes of preserved and live specimens. This is because it allows for 3D visualization of biological structures, which can be done with tissue anatomy of living, preserved and fossilized material. The CT scan process can provide scans of varying resolution (e.g., standard CT, micro-CT, and nano CT volumetric data), for specimens as large as an elephant or as small as an embryo for both mineralized hard and soft tissue anatomy. The previous destructive procedures can be avoided, such as dissecting the specimen, preserving specimens for later examination (Gignac et al., 2016; Metscher, 2009a, 2009b; Neu & Genin, 2014). This is particularly valuable for historical material, delicate specimens, and specimens that may be one-of-a-kind.

Much of our understanding of embryonic development depends on visualization of key morphological traits in different experimental conditions or among species. Effective methods for visualizing these embryonic phenotypes have historically come from visualization techniques such as serial histological sectioning and light microscopy. These methods are known to be time consuming, may destroy the embryonic sample, may only comprise 2-dimensional images, and cannot visualize the inner tissues of the embryo. Because of this, a need for 3D imaging for visualizing embryonic phenotypes is fundamental to future studies. As a process based on producing μCT imaging data sets as 3D volume renderings that depict a full range of 3D phenotypic information and can be easily segmented to for visualization of inner tissues, CT scanning has come to the forefront

for further enhancing the analysis of embryological phenotypes (Ding et al., 2019; Wong et al., 2012).

Digital renderings of desired bone or soft tissue can then be shared with the community using 3D specimen repositories such as Morphosource (Boyer et al., 2016; D.M. et al., 2014) and Sketchfab. Several web-accessible digital libraries for morphological data from X-ray imaging techniques now exist and several methods are now available for visualizing prepared 3D models through web-based interfaces such as Sketchfab (Hagmann, 2018; Nesbit et al., 2020b; Tiznado-Matzner et al., 2019). Furthermore, freely available open-source image reconstruction applications such as 3D Slicer are also available for custom segmentation of data or reconstruction. The 3D models have also been uploaded onto www.anolisevodevo.space along with an interactive learning assignment about the embryonic stages and skull ossification of *Anolis* that will serve as an exercise during in class activities.

3D Models in Education

Many embryology and developmental courses have relied on either precious, but fragile embryos or 2D images on worksheets or textbooks. Replacing damaged specimens can be cost prohibitive for many institutions and instructors, minimizing the learning experience of students. Therefore, traditional teaching methods have included lectures, a text, and 2D images that the students passively label. Approaches that involve such a static style of learning, where opportunities to manipulate actual embryos are limited, particularly in undergraduate classes. With today's technological and pedological innovations, many newer processes have become possible to advance the quality of biological education. Recently, following from the necessity of the COVID pandemic, digital educational

resources have become central in the teaching and learning process (Almarzooq et al., 2020).

Embryonic development is seen by many biology students as difficult and puzzling. As multiple organ systems develop simultaneously is three dimensions, students struggle to conceptualize the dynamic changes that are unfolding. A lack of interactive 3D visualization of embryonic growth processes is one potential explanation. Recent studies have demonstrated significant education value to this inclusion of interactive three-dimensional models in biological education (Chekrouni et al., 2020; Garas et al., 2018; Kazoka et al., 2021). The use of interactive 3D atlas in embryology in classes was proven to improve learning experiences of students (Chekrouni et al., 2020; Garas et al., 2018; Kazoka et al., 2021; Prange-Kiel et al., 2016). Not only this but as a freely available digital model become more available, the more expensive commercially available models, may no longer be needed, increasing the accessibility of these enhanced exercises to a broader audience providing students will access to 3D models can be accomplished in two ways: via interactive virtual models or through 3D printing. Commercial 3D printing companies also provide the opportunity for individuals to upload models and print them for a nominal fee.

I designed an assignment to help students learn embryology which can take advantage of either of these options. The assignment is split into three parts: the body, face, and skull development. Students interact with 3D printed models of the body and head the embryonic *A. sagrei.* To further increase accessibility, my assignment is integrated with the website www.anolisevodevo.space for additional support in using the 3D models. For the skull portion of the assignment, the student will use the www.anolisevodevo.space website

interact with 3D models of different stages of the skull. In all three parts, students would then draw out and label key morphological traits that the students would be able to observe, not in a 2D static picture, but in a 3-dimensional view of the embryo. In addition to the models, the learning objectives are also reached through drawing, another proven method that increases student learning (Garas et al., 2018; Kazoka et al., 2021). This 3-part assignment would go be used in practical classes, so that students could learn embryology using 3D models.

CHAPTER 6

CONCLUSION

In this thesis I report the post-ovipositional development of the *A. sagrei* based on external morphological characters and ossification patterns. This work compliments and expands to the previous *A. sagrei* staging series which used only 2D images (Sanger et al., 2008). I have implemented non-destructive µCT scanning techniques for embryological characterization. I tracked limb, craniofacial, and brain development. I also described cranial ossification sequence since a complete morphological description of the embryonic skull is still lacking for most lizard families, including anoles. Furthermore, I have described the developmental stage where early ossification of craniofacial tissues begins. The data generated, such as images and 3D mesh files has been uploaded for global exploration, download, and 3D printing on websites such as: www.anolisevodevo.space, Morphosource, and Sketchfab. Additionally, the data generated is another great resource for future evolutionary and developmental investigations in squamates and the continued study of *A. sagrei* as a model for evo-devo.

I have also created a learning activity that builds upon the interactive 3D models I created for the scientific community. These 3D models aim to enhance the embryology education for levels appropriate for early undergraduate students. For that, I created 60 interactive 3D models encompassing the body, face, and skull of the embryonic staging series. Because the interactive models encompass three parts, the assignment is also split into those respective parts. Students

interact with 3D printed models of the body and head the embryonic *A. sagrei* and use a web-based interface to interact with the 3D rendered models of the skull. My assignment is integrated with the website www.anolisevodevo.space for additional support in using the 3D models. Following this, students will be able to apply what they have learned to the development of other amniotes, in particular with development model systems and human development.

BIBLIOGRAPHY

Alföldi, J., Di Palma, F., Grabherr, M., Williams, C., Kong, L., Mauceli, E., Russell, P., Lowe, C. B., Glor, R. E., Jaffe, J. D., Ray, D. A., Boissinot, S., Shedlock, A. M., Botka, C., Castoe, T. A., Colbourne, J. K., Fujita, M. K., Moreno, R. G., Ten Hallers, B. F., Heiman, D., Janes, D. E., Johnson, J., De Jong, P. J., Koriabine, M. Y., Lara, M., Novick, P. A., Organ, C. L., Peach, S. E., Poe, S., Pollock, D. D., De Queiroz, K., Sanger, T., Searle, S., Smith, J. D., Smith, Z., Swofford, R., Turner-Maier, J., Wade, J., Young, S., Zadissa, A., Edwards, S. V., Glenn, T. C., Schneider, C.J., Losos, J. B., Lander, E. S., Breen, M., Ponting, C. P., & Lindblad-Toh, K. (2011). The genome of the green anole lizard and a comparative analysis with birds and mammals. *Nature*, *477*(7366). https://doi.org/10.1038/nature10390

Arey, L. B. (1974). Developmental anatomy. *Science Education*, *7*(695). https://doi.org/10.1002/sce.3730320162

Arnaout, B., Lantigua, K. E., MacKenzie, E. M., McKinnell, I. W., & Maddin, H. C. (2021). Development of the chicken skull: a complement to the external staging table of Hamburger and Hamilton. *Anatomical Record*, 304(12), 2726-2740. https://doi.org/10.1002/ar.24603

Backhouse, M., Fitzpatrick, M., Hutchinson, J., Thandi, C. S., & Keenan, I. D. (2017). Improvements in anatomy knowledge when utilizing a novel cyclical "observe-reflect-draw-edit-repeat" learning process. *Anatomical Sciences Education*, *10*(1). https://doi.org/10.1002/ase.1616

Bassett, A. R., Tibbit, C., Ponting, C. P., & Liu, J. L. (2013). Highly efficient targeted mutagenesis of *Drosophila* with the CRISPR/Cas9 system. *Cell Reports*, *4*(1). https://doi.org/10.1016/j.celrep.2013.06.020

Bellairs, R., & Osmond, M. (2014). Atlas of chick development: third edition. *Atlas of Chick Development: Third Edition*. https://doi.org/10.1016/C2010-0-65149-2

Benton, M. J., Donoghue, P. C. J., Asher, R. J., Friedman, M., Near, T. J., & Vinther, J. (2015). Constraints on the timescale of animal evolutionary history. *Palaeontologia Electronica*, 18(1). https://doi.org/10.26879/424

Berquist, R. M., Gledhill, K. M., Peterson, M. W., Doan, A. H., Baxter, G. T., Yopak, K. E., Kang, N., Walker, H. J., Hastings, P. A., & Frank, L. R. (2012). The digital fish library:

using MRI to digitize, database, and document the morphological diversity of fish. *PLoS ONE*, *7*(4). https://doi.org/10.1371/journal.pone.0034499

Beuttell, K., & Losos, J. B. (1999). Ecological morphology of Caribbean anoles. *Herpetological Monographs*, *13*, 1–28. https://doi.org/10.2307/1467059

Bininda-Emonds, O. R. P., Cardillo, M., Jones, K. E., MacPhee, R. D. E., Beck, R. M. D., Grenyer, R., Price, S. A., Vos, R. A., Gittleman, J. L., & Purvis, A. (2007). The delayed rise of present-day mammals. *Nature*, *446*(7135), 507–512. https://doi.org/10.1038/nature05634

Boback, S. M., Dichter, E. K., & Mistry, H. L. (2012). A developmental staging series for the African house snake, *Boaedon (Lamprophis) fuliginosus*. *Zoology*, *115*(1), 38–46. https://doi.org/10.1016/j.zool.2011.09.001

Bowler, P. J. (1996). *Life's splendid drama : evolutionary biology and the reconstruction of life's ancestry, 1860-1940* [Book]. University of Chicago Press.

Boyer, D. M., Kaufman, S., Gunnel, G. F., Rosenberger, A. L. (2014). Managing 3D digital data sets of morphology: morphosource is a new project-based data archiving and distribution tool. *American Journal of Physical Anthropology*, 153, 84-84.

Boyer, D. M., Gunnell, G. F., Kaufman, S., & McGeary, T. M. (2016). Morphosource: archiving and sharing 3-d digital specimen data. *The Paleontological Society Papers*, *22*. https://doi.org/10.1017/scs.2017.13

Burke, A. C. (1989). Development of the turtle carapace: implications for the evolution of a novel bauplan. *Journal of Morphology*, *199*(3). https://doi.org/10.1002/jmor.1051990310

Burke, A. C. (1991). The development and evolution of the turtle body plan: inferring intrinsic aspects of the evolutionary process from experimental embryology. *Integrative and Comparative Biology*, *31*(4). https://doi.org/10.1093/icb/31.4.616

Campbell-Staton, S. C., Cheviron, Z. A., Rochette, N., Catchen, J., Losos, J. B., & Edwards, S. V. (2017). Winter storms drive rapid phenotypic, regulatory, and genomic shifts in the green anole lizard. *Science*, *357*(6350). https://doi.org/10.1126/science.aam5512

Carroll, S. B., Weatherbee, S. D., & Langeland, J. A. (1995). Homeotic genes and the regulation and evolution of insect wing number. *Nature*, *375*(6526). https://doi.org/10.1038/375058a0

Carroll, S. B., Grenier, J. K., & Weatherbee, S. D. (2005). *From DNA to diversity: molecular genetics and the evolution of animal design* [Book]. Blackwell. https://doi.org/10.1038/sj.hdy.6800154

Carroll, S. B. (2008). Evo-devo and an expanding evolutionary synthesis: a genetic theory of morphological evolution. *Cell*, *134*(1), 25–36. https://doi.org/10.1016/j.cell.2008.06.030

Chang, C., Wu, P., Baker, R. E., Maini, P. K., Alibardi, L., & Chuong, C. M. (2009). Reptile scale paradigm: evo-devo, pattern formation and regeneration. *International Journal of Developmental Biology*, *53*(5–6), 813–826. https://doi.org/10.1387/ijdb.072556cc

Chekrouni, N., Kleipool, R. P., & de Bakker, B. S. (2020). The impact of using three-dimensional digital models of human embryos in the biomedical curriculum. *Annals of Anatomy*, *227*. https://doi.org/10.1016/j.aanat.2019.151430

Chen, Y.H., Huang, S.-P., Chang, M.-H., & Tu, M.C. (2010). Thermal effects on embryogenesis and hatchlings of the grass lizard *Takydromus stejnegeri* (squamata: *Lacertidae*) and implications of their potential for limiting its altitudinal distribution in Taiwan. *Zoological Studies*. 49, 374-380.

Cleary, J. O., Modat, M., Norris, F. C., Price, A. N., Jayakody, S. A., Martinez-Barbera, J. P., Greene, N. D. E., Hawkes, D. J., Ordidge, R. J., Scambler, P. J., Ourselin, S., & Lythgoe, M. F. (2011). Magnetic resonance virtual histology for embryos: 3D atlases for automated high-throughput phenotyping. *NeuroImage*, *54*(2), 769–778. https://doi.org/10.1016/j.neuroimage.2010.07.039

Degani, G. (2015). Life cycle of tree frogs (*Hyla savygnyi*) in semi-arid habitats in northern Israel. *International Journal of Biology*, *8*(1), 17. https://doi.org/10.5539/ijb.v8n1p17

Degenhardt, K., Wright, A. C., Horng, D., Padmanabhan, A., & Epstein, J. A. (2010). Rapid three-dimensional phenotyping of cardiovascular development in mouse embryos by micro-CT with iodine staining. *Circulation Cardiovascular Imaging*, *3*(3), 314–322. https://doi.org/10.1161/CIRCIMAGING.109.918482.Rapid

Dias, M. S., & Schoenwolf, G. C. (1990). Formation of ectopic neuroepithelium in chick blastoderms: age-related capacities for induction and self-differentiation following transplantation of quail Hensen's nodes. *The Anatomical Record*, *228*(4). https://doi.org/10.1002/ar.1092280410

Diaz, R. E., Bertocchini, F., & Trainor, P. A. (2017). Lifting the veil on reptile embryology: the veiled chameleon (*Chamaeleo calyptratus*) as a model system to study reptilian development. *Methods in Molecular Biology*, 1650, 269–284. https://doi.org/10.1007/978-1-4939-7216-6_18

Ding, Y., Vanselow, D. J., Yakovlev, M. A., Katz, S. R., Lin, A. Y., Clark, D. P., Vargas, P., Xin, X., Copper, J. E., Canfield, V. A., Ang, K. C., Wang, Y., Xiao, X., De Carlo, F., van Rossum, D. B., La Riviere, P., & Cheng, K. C. (2019). Computational 3D histological phenotyping of whole zebrafish by x-ray histotomography. *eLife*, *8*, e44898. https://doi.org/10.7554/eLife.44898

Downs, K. M., & Davies, T. (1993). Staging of gastrulating mouse embryos by morphological landmarks in the dissecting microscope. *Development*, *118*(4), 1255–1266.

Dunmore-Buyze, P. J., Tate, E., Xiang, F. L., Detombe, S. A., Nong, Z., Pickering, J. G., & Drangova, M. (2014). Three-dimensional imaging of the mouse heart and vasculature using micro-CT and whole-body perfusion of iodine or phosphotungstic acid. *Contrast Media and Molecular Imaging*, *9*(5). https://doi.org/10.1002/cmmi.1588

Eckalbar, W. L., Lasku, E., Infante, C. R., Elsey, R. M., Markov, G. J., Allen, A. N., Corneveaux, J. J., Losos, J. B., DeNardo, D. F., Huentelman, M. J., Wilson-Rawls, J., Rawls, A., & Kusumi, K. (2012). Somitogenesis in the anole lizard and alligator reveals evolutionary convergence and divergence in the amniote segmentation clock. *Developmental Biology*, *363*(1). https://doi.org/10.1016/j.ydbio.2011.11.021

Eichberger, G., Perry, C. N., Walker, H. J., Hastings, P., Linsen, L., & Frank, L. R. (2006). Interactive 3D graphics for web-based data analysis and visualization for the digital fish library (DFL). *ACM SIGGRAPH 2006 Research Posters, SIGGRAPH 2006*. https://doi.org/10.1145/1179622.1179818

Fedorov A., Beichel R., Kalpathy-Cramer J., Finet J., Fillion-Robin J-C., Pujol S., Bauer C., Jennings D., Fennessy F.M., Sonka M., Buatti J., Aylward S.R., Miller J.V., Pieper S., K. R. (2012). 3D Slicer as an image computing platform for the quantitative imaging network. *Magnetic Resonance Imaging*, *30*(9), 1323–1341. https://doi.org/10.1016/j.mri.2012.05.001

Fredieu, J. R., Kerbo, J., Herron, M., Klatte, R., & Cooke, M. (2015). Anatomical models: a digital revolution. *Medical Science Educator* 25(2), 183–194. https://doi.org/10.1007/s40670-015-0115-9

Garas, M., Vaccarezza, M., Newland, G., McVay-Doornbusch, K., & Hasani, J. (2018). 3D-Printed specimens as a valuable tool in anatomy education: a pilot study. *Annals of Anatomy*, *219*, 57–64. https://doi.org/10.1016/j.aanat.2018.05.006

Garcia, G. R., Noyes, P. D., & Tanguay, R. L. (2016). Advancements in zebrafish applications for 21st century toxicology. *Pharmacology and Therapeutics* (Vol. 161). https://doi.org/10.1016/j.pharmthera.2016.03.009

Geneva, A. J., Park, S., Bock, D., Mello, P. de, Sarigol, F., Tollis, M., Donihue, C.,

Reynolds, R. G., Feiner, N., Rasys, A. M., Lauderdale, J. D., Minchey, S. G., Alcala, A. J., Infante, C. R., Kolbe, J. J., Schluter, D., Menke, D. B., & Losos, J. B. (2021). Chromosome-scale genome assembly of the brown anole (*Anolis sagrei*), a model species for evolution and ecology. *BioRxiv*.

Gignac, P. M., & Kley, N. J. (2014). Iodine-enhanced micro-CT imaging: methodological refinements for the study of the soft-tissue anatomy of post-embryonic vertebrates. *Journal of Experimental Zoology Part B: Molecular and Developmental Evolution*, *322*(3), 166–176. https://doi.org/10.1002/jez.b.22561

Gignac, P. M., Kley, N. J., Clarke, J. A., Colbert, M. W., Morhardt, A. C., Cerio, D., Cost, I. N., Cox, P. G., Daza, J. D., Early, C. M., Echols, M. S., Henkelman, R. M., Herdina, A. N., Holliday, C. M., Li, Z., Mahlow, K., Merchant, S., Mueller, J., Orsbon, C. P., Paluh, D. J., Thies, M. L., Tsai, H. P., & Witmer, L. M. (2016). Diffusible iodine-based contrast-enhanced computed tomography (diceCT): an emerging tool for rapid, high-resolution, 3-D imaging of metazoan soft tissues. Journal of Anatomy, 228, 889–909. https://doi.org/10.1111/joa.12449

Gilbert, S. F., Loredo, G. A., Brukman, A., & Burke, A. C. (2001). Morphogenesis of the turtle shell: The development of a novel structure in tetrapod evolution. *Evolution and Development*, *3*(2). https://doi.org/10.1046/j.1525-142X.2001.003002047.x

Gilles, A. F., & Averof, M. (2014). Functional genetics for all: engineered nucleases, CRISPR and the gene editing revolution. *EvoDevo*, *5*(1). https://doi.org/10.1186/2041-9139-5-43

Giribet, G. (2010). A new dimension in combining data? The use of morphology and phylogenomic data in metazoan systematics. *Acta Zoologica*, *91*(1). https://doi.org/10.1111/j.1463-6395.2009.00420.x

Glossip, D., & Losos, J. B. (1997). Ecological correlates of number of subdigital lamellae in anoles. *Herpetologica*, *53*(2).

Gray, J. A., Sherratt, E., Hutchinson, M. N., & Jones, M. E. H. (2019). Changes in ontogenetic patterns facilitate diversification in skull shape of Australian agamid lizards. *BMC Evolutionary Biology*, *19*(1). https://doi.org/10.1186/s12862-018-1335-6

Gredler, M. L., Larkins, C. E., Leal, F., Lewis, A. K., Herrera, A. M., Perriton, C. L., Sanger, T. J., & Cohn, M. J. (2014). Evolution of external genitalia: insights from reptilian development. *Sexual Development*, *8*(5). https://doi.org/10.1159/000365771

Gredler, M. L., Sanger, T. J., & Cohn, M. J. (2015). Development of the cloaca, hemipenes, and hemiclitores in the green anole, *Anolis carolinensis*. *Sexual Development*, *9*(1). https://doi.org/10.1159/000363757

Griffing, A. H., Sanger, T. J., Daza, J. D., Nielsen, S. V., Pinto, B. J., Stanley, E. L., & Gamble, T. (2019). Embryonic development of a parthenogenetic vertebrate, the mourning gecko (*Lepidodactylus lugubris*). *Developmental Dynamics*, *248*(11), 1070–1090. https://doi.org/10.1002/dvdy.72

Gorman, G. C., & Hillman, S. (1977). Physiological basis for climatic niche partitioning in two species of Puerto Rican *Anolis* (reptilia, *Lacertilia, Iguanidae*). *Journal of Herpetology*, *11*(3). https://doi.org/10.2307/1563246

Gould, S. J. (1977). *Ontogeny and phylogeny* [Book]. Belknap Press of Harvard University Press.

Gould, S. J. (1982). Change in developmental timing as a mechanism of macroevolution. *Evolution and Development. Report of the Dahlem Workshop, Berlin, 1981*. https://doi.org/10.1007/978-3-642-45532-2_16

Gunderson, A. R., & Leal, M. (2012). Geographic variation in vulnerability to climate warming in a tropical Caribbean lizard. *Functional Ecology*, *26*(4). https://doi.org/10.1111/j.1365- 2435.2012.01987.x

Hagmann, D. (2018). Reflections on the use of social networking sites as an interactive tool for data dissemination in digital archaeology. *Interdisciplinaria Archaeologica, 9*(1). https://doi.org/10.24916/iansa.2018.1.1

Hall, B. K. (1992). *Evolutionary developmental biology* (1st ed.) [Book]. Chapman & Hall.

Hall, B. K. (1999). Building vertebrate embryos: heads and tails. *Evolutionary Developmental Biology*. https://doi.org/10.1007/978-94-011-3961-8_10

Hall, B. K. (2002). Palaeontology and evolutionary developmental biology: a science of the nineteenth and twenty-first centuries. *Palaeontology*, *45*(4), 647–669. https://doi.org/10.1111/1475-4983.00253

Hall, B. K. (2003). Evo-Devo: evolutionary developmental mechanisms. *International Journal of Developmental Biology*, *47*(7–8), 491–495. https://doi.org/10.1387/ijdb.14756324

Hall, B. K. (2012). Evolutionary developmental biology (evo-devo): past, present, and future. *Evolution: Education and Outreach*, *5*(2), 184–193. https://doi.org/10.1007/s12052-012- 0418-x

Hamburger, V., & Hamilton, H. L. (1951). A series of normal stages in the development of the chick embryo. *Journal of Morphology, 88(1),* 48–92.

Harris, L. D.; Robb, R. A.; Yuen, T. S.; Ritman, E. L. (1979). Display and visualization of three-dimensional reconstructed anatomic morphology. *Journal of Computer Assisted Tomography*, 3(4), 439–446. https://doi.org/10.1097/00004728-197908000-00002

Hatlauf, J., Krendl, L. M., Tintner, J., Griesberger, P., Heltai, M., Markov, G., Viranta, S., & Hackländer, K. (2021). The canine counts! Significance of a craniodental measure to describe sexual dimorphism in canids: golden jackals (*Canis aureus*) and African wolves (*Canis lupaster*). *Mammalian Biology*, *101*(6). https://doi.org/10.1007/s42991-021-00133-2

Hedges, S. B. (2012). Amniote phylogeny and the position of turtles. *BMC Biology*, *10*(64). https://doi.org/10.1186/1741-7007-10-64

Hertz, P. E., Arce-Hernandez, A., Ramirez-Vazquez, J., Tirado-Rivera, W., & Vazquez-Vives, L. (1979). Geographical variation of heat sensitivity and water loss rates in the tropical lizard, *Anolis gundlachi*. *Comparative Biochemistry and Physiology -- Part A: Physiology*, *62*(4). https://doi.org/10.1016/0300-9629(79)90033-1

Holliday, C. M., Tsai, H. P., Skiljan, R. J., George, I. D., & Pathan, S. (2013). A 3D interactive model and atlas of the jaw musculature of *Alligator mississippiensis*. *PLoS ONE*, *8*(6). https://doi.org/10.1371/journal.pone.0062806

Hopwood N. (2007). A history of normal plates, tables and stages in vertebrate embryology. *The International journal of developmental biology*, *51*(1), 1–26. https://doi.org/10.1387/ijdb.062189nh.

Huey, R. B., & Bennett, A. F. (1987). Phylogenetic studies of coadaptation: preferred temperatures versus optimal performance temperatures of lizards. *Evolution*, *41*(5). https://doi.org/10.1111/j.1558-5646.1987.tb05879.x

Hunter, P. (2008). The paradox of model organisms. The use of model organisms in research will continue despite their shortcomings. *EMBO Reports*, *9*(8), 717–720. https://doi.org/10.1038/embor.2008.142

Hutchins, E. D., Markov, G. J., Eckalbar, W. L., George, R. M., King, J. M., Tokuyama, M. A., Geiger, L. A., Emmert, N., Ammar, M. J., Allen, A. N., Siniard, A. L., Corneveaux, J. J., Fisher, R. E., Wade, J., DeNardo, D. F., Rawls, J. A., Huentelman, M. J., Wilson-Rawls, J., & Kusumi, K. (2014). Transcriptomic analysis of tail regeneration in the lizard *Anolis carolinensis* reveals activation of conserved vertebrate developmental and repair mechanisms. *PLoS ONE*, *9*(8). https://doi.org/10.1371/journal.pone.0105004

Hutchins, E. D., Eckalbar, W. L., Wolter, J. M., Mangone, M., & Kusumi, K. (2016). Differential expression of conserved and novel microrna during tail regeneration in the lizard *Anolis carolinensis*. *BMC Genomics*, *17*(1).

https://doi.org/10.1186/s12864-016- 2640-3

Infante, C. R., Mihala, A. G., Park, S., Wang, J. S., Johnson, K. K., Lauderdale, J. D., & Menke, D. B. (2015). Shared enhancer activity in the limbs and phallus and functional divergence of a limb-genital cis-regulatory element in snakes. *Developmental Cell*, *35*(1). https://doi.org/10.1016/j.devcel.2015.09.003

Irschick, D. J., & Losos, J. B. (1998). A comparative analysis of the ecological significance of maximal locomotor performance in Caribbean *Anolis* lizards. In *Evolution*, 52(1). https://doi.org/10.1111/j.1558-5646.1998.tb05155.x

Irschick, D. J., & Losos, J. B. (1999). Do lizards avoid habitats in which performance is submaximal? The relationship between sprinting capabilities and structural habitat use in Caribbean anoles. *American Naturalist*, *154*(3). https://doi.org/10.1086/303239

Jenner, R. A., & Wills, M. A. (2007). Opinion: The choice of model organisms in evo-devo. In *Nature Reviews Genetics*, 8(4). https://doi.org/10.1038/nrg2062

Jensen, B., van den Berg, G., van den Doel, R., Oostra, R. J., Wang, T., & Moorman, A. F. M. (2013). Development of the hearts of lizards and snakes and perspectives to cardiac evolution. *PLoS ONE*, *8*(6). https://doi.org/10.1371/journal.pone.0063651

Kaliontzopoulou, A., Carretero, M. A., & Llorente, G. A. (2007). Multivariate and geometric morphometrics in the analysis of sexual dimorphism variation in *Podarcis* lizards. *Journal of Morphology*, *268*(2). https://doi.org/10.1002/jmor.10494

Kazoka, D., Pilmane, M., & Edelmers, E. (2021). Facilitating student understanding through incorporating digital images and 3D-printed models in a human anatomy course. *Education Sciences*, *11*(8). https://doi.org/10.3390/educsci11080380

Kimmel C, Ballard W, Kimmel S, Ullmann B, S. T. (1995). Stages of embryonic development of the zebrafish. *Developmental Dynamics*, *18*(4). https://doi.org/10.3390/ijms18040817

Koshiba-Takeuchi, K., Mori, A. D., Kaynak, B. L., Cebra-Thomas, J., Sukonnik, T., Georges, R. O., Latham, S., Beck, L., Henkelman, R. M., Black, B. L., Olson, E. N., Wade, J., Takeuchi, J. K., Nemer, M., Gilbert, S. F., & Bruneau, B. G. (2009). Erratum: reptilian heart development and the molecular basis of cardiac chamber evolution. *Nature,* 461, 95-98. https://doi.org/10.1038/nature08464

Kusumi, K., May, C. M., & Eckalbar, W. L. (2013). A large-scale view of the evolution of amniote development: Insights from somitogenesis in reptiles. *Current Opinion in Genetics and Development*, *23*(4), 491–497. https://doi.org/10.1016/j.gde.2013.02.011

Langerhans, R. B., Knouft, J. H., & Losos, J. B. (2006). Shared and unique features of diversification in greater Antillean *Anolis* ecomorphs. *Evolution*, *60*(2). https://doi.org/10.1111/j.0014-3820.2006.tb01112.x

Laurin, M., & Reisz, R. R. (1995). A reevaluation of early amniote phylogeny. *Zoological Journal of the Linnean Society*, *113*(2). https://doi.org/10.1006/zjls.1995.0007

Lautenschlager, S., Bright, J. A., & Rayfield, E. J. (2014). Digital dissection - using contrast- enhanced computed tomography scanning to elucidate hard- and soft-tissue anatomy in the Common Buzzard *Buteo buteo*. *Journal of Anatomy*, *224*(4), 412–431. https://doi.org/10.1111/joa.12153

Leal, F., & Cohn, M. J. (2016). Loss and re-emergence of legs in snakes by modular evolution of sonic hedgehog and HOXD enhancers. *Current Biology*, *26*(21), 2966–2973. https://doi.org/10.1016/j.cub.2016.09.020

Lesciotto, K. M., Motch Perrine, S. M., Kawasaki, M., Stecko, T., Ryan, T. M., Kawasaki, K., & Richtsmeier, J. T. (2020). Phosphotungstic acid-enhanced microct: optimized protocols for embryonic and early postnatal mice. *Developmental Dynamics*, *249*(4), 573–585. https://doi.org/10.1002/dvdy.136

Losos, J. B. (1990). Ecomorphology, performance capability, and scaling of West Indian *Anolis* lizards: an evolutionary analysis. *Ecological Monographs*, *60*(3). https://doi.org/10.2307/1943062

Losos, J. B. (1990). The evolution of form and function: morphology and locomotor performance in West Indian *Anolis* lizards. *Evolution*, *44*(5). https://doi.org/10.1111/j.1558- 5646.1990.tb05225.x

Losos, J. B. (1992). The evolution of convergent structure in Caribbean *Anolis* communities. *Systematic Biology*, *41*(4), 403–420.

Losos, J. B. (1994). Integrative approaches to evolutionary ecology: *Anolis* lizards as model systems. In *Annual Review of Ecology and Systematics* (Vol. 25). https://doi.org/10.1146/annurev.es.25.110194.002343

Losos, J. B., & Sinervo, B. (1989). The effects of morphology and perch diameter on sprint performance of *Anolis* lizards. *Journal of Experimental Biology*, *145*. https://doi.org/10.1242/jeb.145.1.23

Losos, J. B. (2009). *Lizards in an evolutionary tree: ecology and adaptive radiation of anoles* [Book].Berkley: University of California Press.

Losos, J. B., & Ricklefs, R. E. (2009). Adaptation and diversification on islands. *Nature*, *457*(7231), 830–836. https://doi.org/10.1038/nature07893

Losos, J. B., & Schneider, C. J. (2009). *Anolis* lizards. *Current Biology*, *19*(8), R316–R318. https://doi.org/10.1016/j.cub.2009.02.017

McCusker, C., & Gardiner, D. M. (2011). The axolotl model for regeneration and aging research: a mini-review. *Gerontology* (Vol. 57, Issue 6, pp. 565–571). https://doi.org/10.1159/000323761

McDowell, E. M., & Trump, B. F. (1976). Histologic fixatives suitable for diagnostic light and electron microscopy. *Archives of Pathology and Laboratory Medicine*, 100(8), 405-414.

McKinney, M. L. (1991). *Heterochrony: the evolution of ontogeny* [Book]. Plenum Press.

Metscher, B. D. (2009a). Micro CT for developmental biology: a versatile tool for high-contrast 3D imaging at histological resolutions. *Developmental Dynamics*, *238*(3), 632–640. https://doi.org/10.1002/dvdy.21857

Metscher, B. D. (2009b). Micro CT for comparative morphology: simple staining methods allow high-contrast 3D imaging of diverse non-mineralized animal tissues. *BMC Physiology*, *9*(1), 1–14. https://doi.org/10.1186/1472-6793-9-11

Metscher, B. D., & Müller, G. B. (2011). MicroCT for molecular imaging: quantitative visualization of complete three-dimensional distributions of gene products in embryonic limbs. *Developmental Dynamics*, *240*(12). https://doi.org/10.1002/dvdy.22783

Milinkovitch, M. C., & Tzika, A. (2007). Escaping the mouse trap: the selection of new evo-devo model species. *Journal of Experimental Zoology Part B: Molecular and Developmental Evolution*, *308*(4), 337–346. https://doi.org/10.1002/jez.b.21180

Mizutani, R., & Suzuki, Y. (2012). X-ray microtomography in biology. *Micron*, 43(2–3). https://doi.org/10.1016/j.micron.2011.10.002

Moczek, A. P., Sears, K. E., Stollewerk, A., Wittkopp, P. J., Diggle, P., Dworkin, I., Ledon-Rettig, C., Matus, D. Q., Roth, S., Abouheif, E., Brown, F. D., Chiu, C. H., Cohen, C. S.,Tomaso, A. W., Gilbert, S. F., Hall, B., Love, A. C., Lyons, D. C., Sanger, T. J., Smith, J., Specht, C., Vallejo-Marin, M., & Extavour, C. G. (2015). The significance and scope of evolutionary developmental biology: a vision for the 21st century. *Evolution & development*, *17*(3), 198–219. https://doi.org/10.1111/ede.12125

Muñoz, M. M., Stimola, M. A., Algar, A. C., Conover, A., Rodriguez, A. J., Landestoy, M. A., Bakken, G. S., & Losos, J. B. (2014). Evolutionary stasis and lability in thermal physiology in a group of tropical lizards. *Proceedings of the Royal Society B: Biological Sciences*, *281*(1778). https://doi.org/10.1098/rspb.2013.2433

Murta-Fonseca, R. A., Machado, A., Lopes, R. T., & Fernandes, D. S. (2019). Sexual

dimorphism in *Xenodon neuwiedii* skull revealed by geometric morphometrics (Serpentes; Dipsadidae). *Amphibia Reptilia*. https://doi.org/10.1163/15685381-20191147

Narzary, J., & Bordoloi, S. (2013). Study of normal development and external morphology of tadpoles of *Microhyla Ornata* and *Uperodon Globulosus* of the family *Microhylidae* (amphibia: *Anura*). *International Journal of Advanced Biological Research*, *3*(1), 61–73.

Nesbit, P. R., Boulding, A. D., Hugenholtz, C. H., Durkin, P. R., & Hubbard, S. M. (2020). Visualization and sharing of 3D digital outcrop models to promote open science. *GSA Today*, *30*(6). https://doi.org/10.1130/GSATG425GW.1

Neu, C. P., & Genin, G. M. (2014). *Handbook of Imaging in Biological Mechanics* [Book]. CRC Press.

Noro, M., Uejima, A., Abe, G., Manabe, M., & Tamura, K. (2009). Normal developmental stages of the Madagascar ground gecko *Paroedura pictus* with special reference to limb morphogenesis. *Developmental Dynamics*, *238*(1). https://doi.org/10.1002/dvdy.21828

O'Leary. M.A., & Kaufman, S. (2011). Morphobank: phylophenomics in the "cloud." *Cladistics*, 27 (5), 529-537. https://doi.org/10.1111/j.1096-0031.2011.00355.x

Oliveira, L. R., Hingst-Zaher, E., & Morgante, J. S. (2005). Size and shape sexual dimorphism in the skull of the South American fur seal, *Arctocephalus australis* (Zimmermann, 1783) (carnivora: *Otariidae*). *Latin American Journal of Aquatic Mammals*, *4*(1). https://doi.org/10.5597/lajam00067

Ollonen, J., Da Silva, F. O., Mahlow, K., & Di-Poï, N. (2018). Skull development, ossification pattern, and adult shape in the emerging lizard model organism *Pogona vitticeps*: A comparative analysis with other squamates. *Frontiers in Physiology*, *9*, 1–26. https://doi.org/10.3389/fphys.2018.00278

Parichy, D. M., Elizondo, M. R., Mills, M. G., Gordon, T. N., & Engeszer, R. E. (2009). Normal table of postembryonic zebrafish development: staging by externally visible anatomy of the living fish. *Developmental Dynamics*, *238*(12), 2975–3015. https://doi.org/10.1002/dvdy.22113

Park, S., Infante, C. R., Rivera-Davila, L. C., & Menke, D. B. (2014). Conserved regulation of HOXC11 by PITX1 in *Anolis* lizards. *Journal of Experimental Zoology Part B: Molecular and Developmental Evolution*, *322*(3). https://doi.org/10.1002/jez.b.22554

Pauwels, E., Van Loo, D., Cornillie, P., Brabant, L., & Van Hoorebeke, L. (2013). An

exploratory study of contrast agents for soft tissue visualization by means of high resolution X-ray computed tomography imaging. *Journal of Microscopy*, *250*(1). https://doi.org/10.1111/jmi.12013

Phipps, L. S., Marshall, L., Dorey, K., & Amaya, E. (2020). Model systems for regeneration: *Xenopus*. *Development (Cambridge)*, *147*(6). https://doi.org/10.1242/dev.180844

Piestun, Y., Halevy, O., & Yahav, S. (2009). Thermal manipulations of broiler embryos-The effect on thermoregulation and development during embryogenesis. *Poultry Science*, *88*(12), 2677–2688. https://doi.org/10.3382/ps.2009-00231

Poe, S., & Anderson, C. G. (2019). The existence and evolution of morphotypes in *Anolis* lizards: coexistence patterns, not adaptive radiations, distinguish mainland and island faunas. *PeerJ*, *3*(6), 1–19. https://doi.org/10.7717/peerj.6040

Pointer, D. (2008). Computed tomography (CT) scan image reconstruction on the SRC-7. *SRC Computers, Inc*.

Prange-Kiel, J., Champine, J. G., Winkler, A. J., & Twickler, D. M. (2016). Embryology, anatomy, and radiology of cervical cysts and cleft lip/palate: a team-based learning module for medical students. *MedEdPORTAL,* 12(1). https://doi.org/10.15766/mep_2374- 8265.10484

Prum, R. O., & Brush, A. H. (2002). The evolutionary origin and diversification of feathers. *Quarterly Review of Biology*, 77(3). https://doi.org/10.1086/341993

Raff, R.A. (1996) *The shape of life* [Book]. Chicago: University of Chicago Press.

Ranasinghe, P., Thorn, R. J., Seto, R., Creton, R., Bridges, W. C., Chapman, S. C., & Lee, C. M. (2020). Embryonic exposure to 2,2′,3,5′,6-pentachlorobiphenyl (PCB-95) causes developmental malformations in zebrafish. *Environmental Toxicology and Chemistry*, *39*(1), 162–170. https://doi.org/10.1002/etc.4587

Rand, A. S. (1969). Competitive exclusion among anoles (sauria: *Iguanidae*) on small islands in the West Indies. *Breviora*, *319*.

Rasys, A. M., Park, S., Ball, R. E., Alcala, A. J., Lauderdale, J. D., & Menke, D. B. (2019). CRISPR-Cas9 gene editing in lizards through microinjection of unfertilized oocytes. *Cell reports*, *28*(9), 2288–2292. https://doi.org/10.1016/j.celrep.2019.07.089

Raynaud, A. (1990). Developmental mechanism involved in the embryonic reduction of limbs in reptiles. *International Journal of Developmental Biology*, 34 (1), 233–243. https://doi.org/10.1387/ijdb.2203460

Ritzman, T. B., Stroik, L. K., Julik, E., Hutchins, E. D., Lasku, E., Denardo, D. F., Wilson-Rawls, J., Rawls, J. A., Kusumi, K., & Fisher, R. E. (2012). The gross anatomy of the original and regenerated tail in the green Anole (*Anolis carolinensis*). *Anatomical Record*, *295*(10). https://doi.org/10.1002/ar.22524

Roy, S., & Gatien, S. (2008). Regeneration in axolotls: a model to aim for! *Experimental Gerontology*, 43(11), 968–973. https://doi.org/10.1016/j.exger.2008.09.003

Sanger, T. J., Losos, J. B., & Gibson-Brown, J. J. (2008). A developmental staging series for the lizard genus *Anolis*: a new system for the integration of evolution, development, and ecology. *Journal of Morphology*, *269*, 129–137. https://doi.org/10.1002/jmor.10563

Sanger, T. J., Hime, P. M., Johnson, M. A., Diani, J., & Losos, J. B. (2008). Laboratory protocols for husbandry and embryo collection of *Anolis* lizards. *Herpetological Review*, *39*(1), 58– 63.

Sanger, T. J. (2012). The emergence of squamates as model systems for integrative biology. *Evolution and Development*, *14*(3), 231–233. https://doi.org/10.1111/j.1525-

Sanger, T. J., Sherratt, E., Mcglothlin, J. W., Brodie, E. D., Losos, J. B., & Abzhanov, A. (2013). Convergent evolution of sexual dimorphism in skull shape using distinct developmental strategies. *Evolution*, *67*(8), 2180–2193. https://doi.org/10.1111/evo.12100142X.2012.00541.x

Sanger, T. J., and Kircher, B. K. (2017). Model clades versus model species: *Anolis* lizards as an integrative model of anatomical evolution. *Evolution & Development*, 14(3), 231–233. https://doi.org/10.1007/978-1-4939-7216-6

Sanger, T. J., Kyrkos, J., Lachance, D. J., Czesny, B., & Stroud, J. T. (2018). The effects of thermal stress on the early development of the lizard *Anolis* sagrei. *Journal of Experimental Zoology Part A: Ecological and Integrative Physiology*, *329*(4–5), 244–251. https://doi.org/10.1002/jez.2185

Sanger, T. J., & Rajakumar, R. (2019). How a growing organismal perspective is adding new depth to integrative studies of morphological evolution. *Biological Reviews*, *94*(1), 184– 198. https://doi.org/10.1111/brv.12442

Sanger, T. J., Harding, L., Kyrkos, J., Turnquist, A. J., Epperlein, L., Nunez, S. A., Lachance, D., Dhindsa, S., Stroud, J. T., Diaz, R. E., & Czesny, B. (2021). Environmental thermal stress induces neuronal cell death and developmental malformations in reptiles. *Integrative Organismal Biology*, *3*(1). https://doi.org/10.1093/iob/obab033

Schwarz, T., Kelley, C., Pinkerton, M. E., & Hartup, B. K. (2016). Computed tomographic anatomy and characteristics of respiratory aspergillosis in juvenile whooping cranes. *Veterinary Radiology and Ultrasound*, *57*(1), 16–23. https://doi.org/10.1111/vru.12306

Shi, J. J., Westeen, E. P., & Rabosky, D. L. (2018). Digitizing extant bat diversity: an open-access repository of 3D μCT-scanned skulls for research and education. *PLoS ONE*, *13*(9). https://doi.org/10.1371/journal.pone.0203022

Shi, L., Liu, B., Yu, H., Wei, C., Wei, L., Zeng, L., & Wang, G. (2020). Review of CT image reconstruction open source toolkits. *Journal of X-Ray Science and Technology*, *28*(4), 619– 639. https://doi.org/10.3233/xst-200666

Schoener, T. W. (1988). Testing for non-randomness in sizes and habitats of West Indian lizards: choice of species pool affects conclusions from null models. *Evolutionary Ecology*, *2*(1). https://doi.org/10.1007/BF02071585

Senn, D. G. (1979). Embryonic development of the central nervous system. *Biology of Reptilia*, *9*, 173–244.

Siefferman, L., and G. E. Hill. 2005. Evidence for sexual selection on structural plumage coloration in female eastern bluebirds (*Sialia sialis*). *Evolution,* 59,1819–1828.

Simpson, B. B., & Niklas, K. J. (1997). The evolutionary biology of plants. *Systematic Botany*, *22*(4). https://doi.org/10.2307/2419438

Smith, K. K. (2001). Heterochrony revisited: the evolution of developmental sequences. *Biological Journal of the Linnean Society*, *73*(2). https://doi.org/10.1006/bijl.2001.0535

Storey, K. G., Crossley, J. M., De Robertis, E. M., Norris, W. E., & Stern, C. D. (1992). Neural induction and regionalization in the chick embryo. *Development*, *114*(3). https://doi.org/10.1242/dev.114.3.729

Stern, C. D. (2018). Staging tables for avian embryos: a little history. *International Journal of Developmental Biology*, *62*(1–3), 43–48. https://doi.org/10.1387/ijdb.170299cs

Streit, A., Sockanathan, S., Pérez, L., Rex, M., Scotting, P. J., Sharpe, P. T., Lovell-Badge, R., & Stern, C. D. (1997). Preventing the loss of competence for neural induction: HGF/SF, L5 and Sox-2. *Development*, *124*(6). https://doi.org/10.1242/dev.124.6.1191

Theiler, K. (1972). *The house mouse: development and normal stages from fertilization to 4 weeks of age* [Book]. Springer Verlag.

Tiznado-Matzner, G., Bucarey-Arriagada, S., & Pérez, R. L. (2019). Experience in the creation of an online platform to host three-dimensional models of real anatomical pieces to be shared as open educational resources (OER). *International Journal of*

Morphology, *37*(4). https://doi.org/10.4067/S0717-95022019000401267

Tschopp, P., Sherratt, E., Sanger, T. J., Groner, A. C., Aspiras, A. C., Hu, J. K., Pourquié, O., Gros, J., & Tabin, C. J. (2014). A relative shift in cloacal location repositions external genitalia in amniote evolution. *Nature*, *516*(7531). https://doi.org/10.1038/nature13819

Uetz, P., & Stylianou, A. (2018). The original descriptions of reptiles and their subspecies. *Zootaxa*, *4375*(2), 257–264. https://doi.org/10.11646/zootaxa.4375.2.5

Wagner, G. P., Chiu, C. H., & Laubichler, M. (2000). Developmental evolution as a mechanistic science: the inference from developmental mechanisms to evolutionary processes. *American Zoologist*, *40*(5), 819–831. https://doi.org/10.1093/icb/40.5.819

Wallingford, V. H. (1953). The development of organic iodine compounds as X-ray contrast media. *Journal of the American Pharmaceutical Association*, *42*(12), 721–728. https://doi.org/10.1002/jps.3030421206

Wang, S., Zhao, L., Liu, L., Yang, D., Khatiwada, J. R., Wang, B., & Jiang, J. (2017). A complete embryonic developmental table of *Microhyla fissipes* (Amphibia, *Anura*, *Microhylidae*). *Asian Herpetological Research*, *8*(2), 108–117. https://doi.org/10.16373/j.cnki.ahr.170006

Weatherbee, S. D., Nijhout, H. F., Grunert, L. W., Halder, G., Galant, R., Selegue, J., & Carroll, S. (1999). *Uitrabithorax* function in butterfly wings and the evolution of insect wing patterns. *Current Biology*, 9(3). https://doi.org/10.1016/S0960-9822(99)80064-5

Williams, E. E. (1972). The origin of faunas. evolution of lizard congeners in a complex island fauna: a trial analysis. *Evolutionary Biology*. https://doi.org/10.1007/978-1- 4684-9063-3_3

Williams, E. E. (1983). 15. Ecomorphs, faunas, island size, and diverse end points in island radiations of *Anolis*. *Lizard Ecology* (pp. 326–370). https://doi.org/10.4159/harvard.9780674183384.c18

Wise, P. A. D., Vickaryous, M. K., & Russell, A. P. (2009). An embryonic staging table for in ovo development of *Eublepharis macularius*, the leopard gecko. *Anatomical Record*, *292*(8), 1198–1212. https://doi.org/10.1002/ar.20945

Wong, M. D., Dorr, A. E., Walls, J. R., Lerch, J. P., & Mark Henkelman, R. (2012). A novel 3D mouse embryo atlas based on micro-CT. *Development (Cambridge)*, *139*(17), 3248–3256. https://doi.org/10.1242/dev.082016

Yaryhin, O., Klembara, J., Pichugin, Y., Kaucka, M., & Werneburg, I. (2021). Limb reduction in squamate reptiles correlates with the reduction of the chondrocranium: a

case study on *Serpentiform anguids*. *Developmental Dynamics*, 250(9), 1300-1317. https://doi.org/10.1002/dvdy.307

Ziegler, A., Ogurreck, M., Steinke, T., Beckmann, F., Prohaska, S., & Ziegler, A. (2010). Opportunities and challenges for digital morphology. *Biology Direct*, 5. https://doi.org/10.1186/1745-6150-5-45

VITA

Lilian Epperlein was born in Tarzana, California, and was raised in Cologne, Germany, and moved to the United States in 2006. She attended the University of Arizona, Tempe where she earned a Bachelor of Science in Biology: Genetics and Cells in 2018.

From 2018 she began her Master of Science in Biology at Loyola University Chicago, focusing on the development of Anolis sagrei lizard using CT scanning. This thesis was presented in part at the Society for Integrative and Comparative Biology (SICB 2020). While at Loyola, she also became a co-author on a few papers (Griffing et al., 2021; Sanger et al., 2021), and enjoyed teaching General Biology Laboratory (BIOL 111 and 112).

Currently, Ms. Epperlein is an instructor at Loyola University Chicago.